NAT'L INST. OF STAND & TECH
A11106 137669
NIST
PUBLICATIONS
REFERENCE

# NISTIR 7142

# Triangular Meshing And Volume Determination

Building and Fire Research Laboratory
Gaithersburg, MD 20899

**United States Department of Commerce**
**Technology Administration**
National Institute of Standards and Technology

QC
100
.U56
#7142
2004

# NISTIR 7142

# Triangular Meshing And Volume Determination

Christoph Witzgall
Geraldine S. Cheok

July 2004
Building and Fire Research Laboratory
National Institute of Standards and Technology
Gaithersburg, MD 20899

**U. S. Department of Commerce**
Donald L. Evans, *Secretary*
Technology Administration

Phillip J. Bond, *Under Secretary*
Technology Administration

National Institute of Standards and Technology
Ardent L. Bement, *Director*

## ABSTRACT

Parametric studies are reported which investigate the feasibility and accuracy of calculating volumes from LADAR (laser detection and ranging) scans of artifacts. The Triangulated Irregular Network (TIN) technique was employed to construct the surfaces on which the volume calculation was based. The artifact used was a plywood box of known size and volume. Scans were taken of a tight fitting background screen, with and without the box placed against it. The volume of the box was then recovered as the difference between respective cut or, alternatively, fill volumes. A procedure for determining such cut and fill volumes is described. The representation of point clouds by triangulated surfaces offers several algorithmic options as well as choices of parameters. The sensitivity and accuracy of volume calculations was examined for several alternative algorithmic options and parameter settings.



**Keywords:** approximation, Delaunay, experiments, LADAR, meshing, surface, TIN, triangulation, volume.

# CONTENTS

ABSTRACT ..... iii

CONTENTS ..... v

1. INTRODUCTION ..... 1

2. THE MESHING PROCESS ..... 3
   2.1 Triangulated Irregular Networks (TINs) ..... 4
   2.2 Delaunay Triangulations ..... 5
   2.3 Interpolation and Approximation ..... 6
   2.4 The Insertion Method For Delaunay TINs ..... 7
      2.4.1 Vertex Selection for Approximation ..... 9
      2.4.2 Inserting a Vertex ..... 9

3. POST-PROCESSING PROCEDURES ..... 11
   3.1 Relevant Triangles ..... 11
   3.2 Elevation Adjustment ..... 12
   3.3 Triangulation Adjustment ..... 12
   3.4 Filtering and Screening ..... 13

4. CALCULATING VOLUMES ..... 14
   4.1 Decomposition into Triangular Prismoids ..... 15
   4.2 Floor Determination ..... 17

5. EXPERIMENTAL VOLUME DETERMINATION ..... 19
   5.1 Experiment 1 ..... 22
   5.2 Experiment 2 ..... 26
   5.3 Experiment 3 ..... 28
   5.4 Experiment 4 ..... 29

6. SUMMARY AND CONCLUSIONS ..... 43

REFERENCES ..... 45

# 1. INTRODUCTION

NIST is investigating the utility and accuracy of LADAR (LAser Detection And Ranging) scanning devices for surface recovery with particular emphasis on applications by the construction industry [Cheok et al., 2000]. NIST is also involved in planning a performance evaluation facility for LADAR instruments and associated data processing methods.

As a step towards accuracy assessment, LADAR scans of a plywood box were collected in a laboratory environment. The resulting point clouds were meshed using Triangulated Irregular Network (TIN) techniques as part of the volume calculation. Comparison of that calculated value with a separately measured volume of the box provides an indication of the accuracy of the instrument as well as various methods of data analysis. Of particular interest are the sensitivities of the results to alternate data representations such as choices of the coordinate system and cropping, as well as parameter settings and procedural options included in the meshing algorithm. The volume so calculated was then used to gauge the accuracy of the scanning instrument as well as of the meshing algorithm by comparing it to the separately measured volume. The NIST prototype routine

"*TINvolume*"

was used for both meshing and volume calculations.

The experiment set-up included a screen of two perpendicular rectangular plywood sheets, positioned flush against the faces of the box not visible from instrument position (Fig. 1.1). Scans were taken from the same instrument position and without changing instrument orientation of (*i*) the screen by itself without the box, and (*ii*) the screen with the box. Those two kinds of measurements were then used to determine the volume of the box from the difference between corresponding surfaces.

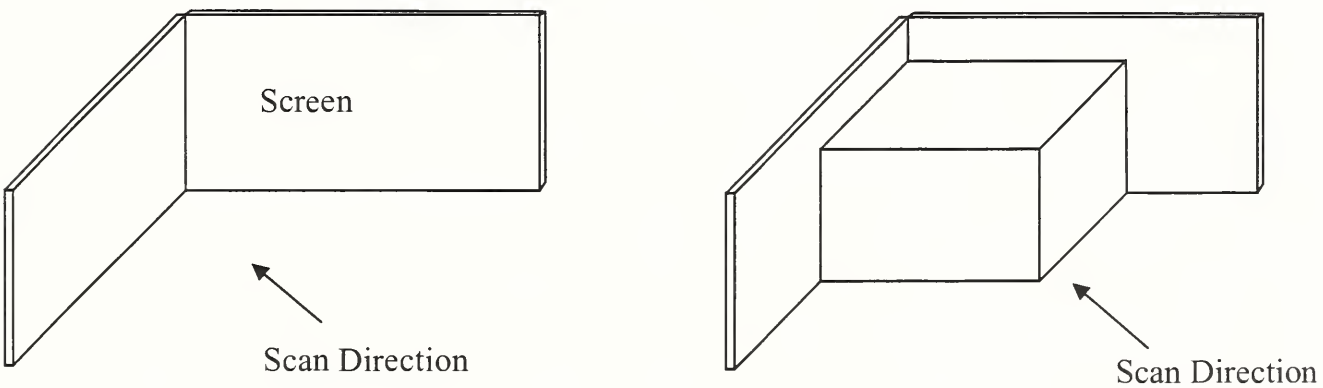


a. Scan with screen only.

b. Scan with box and screen.

Figure 1.1. Experiment Set-up.

A previous report [Witzgall and Cheok 2001] provided a first analysis of scans of the same box taken from four separate locations so as to cover areas occluded by individual scans. In addition to meshing, those experiments required registration, that is, rigid transformation of separate coordinate frames to a common frame. Since the experiments in this report aim to assess the accuracy of meshing techniques, and since registration introduces additional errors, the data collection for the experiments was designed to avoid the need for registration.

The following Chapter 2 provides an overview of the TIN meshing process. For more details, the reader is referred to the report by [Witzgall et al., 2004]. Post-processing procedures, such as elevation and triangulation adjustments are discussed in Chapter 3, and the numerical basis for the volume calculations is presented in Chapter 4. The experiments are reported in Chapter 5.

## 2. THE MESHING PROCESS

A LADAR device gathers 3D data in the form of a

"point cloud",

a collection of 3D locations represented in some coordinate system or "frame." The immediate output will typically be in instrument-centered "polar" coordinates, given by

"angle, angle, distance" $(\varphi, \theta, r)$,

where the angles $\varphi, \theta$ represent instrument settings, and the distance or "range" $r$ is measured. The polar coordinates are commonly converted to "Cartesian" coordinates $(x, y, z)$ centered at the instrument. The coordinate $z$ of such a point is interpreted as its elevation, and the projection $(x, y)$ as its location or

"footprint".

In this report, the data points $P_i$ are assumed to be given in such coordinates,

$$P_i = (x_i, y_i, z_i),$$

with footprints $p_i = (x_i, y_i)$.

In many applications, and often intuitively, the $z$-coordinate of the Cartesian coordinate system is considered as the vertical elevation above a horizontal footprint plane. It is important to realize that the $x, y, z$-coordinate system need not be chosen in this fashion. For instance, the footprint plane may be perpendicular to a scanning direction. In that case, the $z$-coordinate approximates distance from the instrument.

The purpose of meshing is to represent a point cloud by a surface. The surfaces considered in this report (e.g., the surface depicted in Fig. 2.2) satisfy the following

> **Single Elevation Property:** *Any footprint is the projection of a single surface point. In other words, no two different surface points have the same footprint.*

This condition excludes surfaces with undercuts. A surface with this single elevation property is commonly referred to as an

"elevated surface", "parametric surface", or "2.5 D surface".

In typical applications, point clouds are either approximated or interpolated by elevated surfaces. Because of the single elevation property, however, interpolation, that is, the passing of an elevated surface through all data points $P_i$ will not be possible if the point cloud contains what here will be called

"duplicate points",

that is, points with identical footprints but different elevations.

## 2.1 TRIANGULATED IRREGULAR NETWORKS (TINS)

The computational procedures used in this work are based on a particular kind of

"triangular mesh",

referred to [Peucker et al., 1976, 1978] as a

"triangulated irregular network" or "TIN".

Here elevated surfaces are constructed with reference to a

"triangulation"

in the footprint plane (Fig. 2.1).

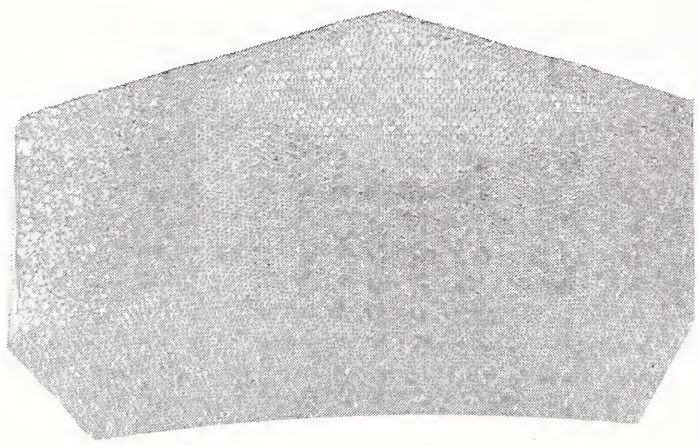

Figure 2.1 A triangulation in a plane perpendicular to the scan direction.

A triangulation is the covering of a 2D region by triangles which do not overlap, that is, have no common points other than vertices and along edges where two triangles join. If elevations $z_v$ are specified at the vertices $q_v = (x_v , y_v)$ of triangles of the TIN, then a TIN surface is created that passes through the corresponding 3D points $Q_v = (x_v , y_v , z_v)$ by elevating each planar triangle $t_k$ with vertices

$$(x_{v_1}, y_{v_1}), (x_{v_2}, y_{v_2}), (x_{v_3}, y_{v_3})$$

to the 3D triangle $T_k$ with the corresponding vertices

$$(x_{v_1}, y_{v_1}, z_{v_1}), (x_{v_2}, y_{v_2}, z_{v_2}), (x_{v_3}, y_{v_3}, z_{v_3}).$$

These elevated triangles then meet along common edges and form a surface in space called a

"TIN surface"

(see Fig. 2.2). The triangulation of the footprints $q_v = (x_v, y_v)$ determines an entire class of TIN surfaces, each of which is defined by the choice of the elevations $z_v$ at the footprints $q_v$. The image of "tent poles" of height $z_v$, supporting the surface at the locations $q_v$, is appropriate. It also suggests the idea of "raising" and "lowering" those "tent poles" so as to best represent the points in the point cloud – a procedure to be discussed in Section 3.2.

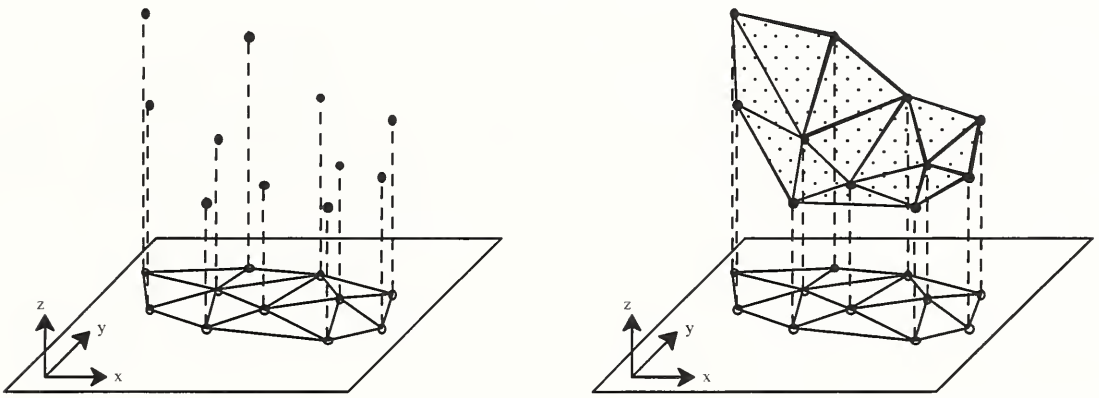


Figure 2.2. A triangulation of data footprints (TIN) and its corresponding TIN surface.

## 2.2 DELAUNAY TRIANGULATIONS

There are many ways of triangulating a set of planar points and, consequently, there are many TIN surfaces through the corresponding sets of 3D vertices. It would therefore be highly desirable to identify a triangulation concept that, given a set of vertices, defines triangulations that are essentially unique, and that would come close to reproducing the intuitive triangulation an analyst would choose. For instance, the occurrence of very long edges and of associated "skinny" triangles will, in general, be reduced. Obviously, such triangles would distort the appearance of any corresponding TIN surface. Such a suitable triangulation concept exists. It is based on the following:

**Empty Circle Criterion:** *No triangulation vertex* $(x_v , y_v)$ *lies in the interior of the circumcircle of any triangle of the triangulation* [Delaunay 1934].

Such triangulations (Fig. 2.3) are widely considered standard, employing the terms

"Delaunay triangulation" or "Delaunay TIN",

and for the corresponding TIN surface, the term

"Delaunay surface".

In fact, the term "TIN" is often used synonymously with "Delaunay TIN". A Delaunay triangulation is, in general, uniquely determined by the empty circle criterion, the exception being the case in which the circumcircle of one of the triangles contains more than three vertices on its periphery. In that exceptional case, the vertices on the periphery of such a triangle determine a convex polygon, which can be subdivided by diagonals in different ways into triangles, and each of these subdivisions is acceptable within a Delaunay triangulation.

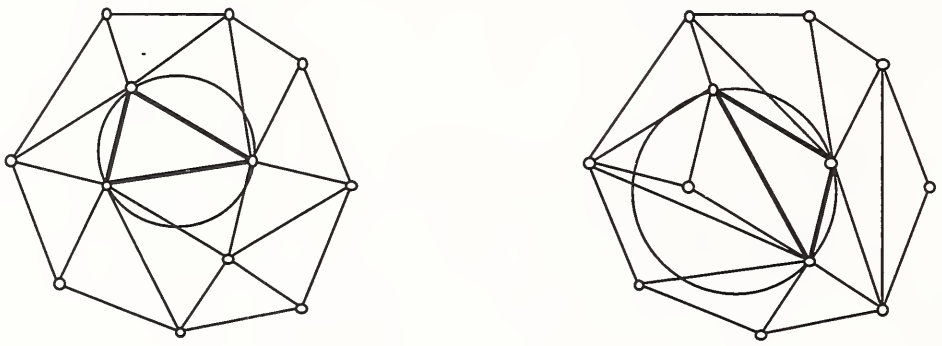

Figure 2.3. Two triangulations of the same set of points. The one on the left is Delaunay.

## 2.3 INTERPOLATION AND APPROXIMATION

So far no assumption has been made about how the footprint points $q_v = (x_v, y_v)$ and their corresponding surface vertices $Q_v = (x_v , y_v , z_v)$ , which describe the TIN surface, are to be chosen. The typical TIN approach, which is also adopted here, is to assume that – with minor exceptions –

*triangulations are constructed from footprints* $p_i = (x_i , y_i)$ *of data points* $P_i = (x_i , y_i , z_i)$ .

If all possible data points are included in the triangulation, then the term

"full triangulation"

is used as opposed to

"partial triangulation",

where a selected subset of the data footprints is triangulated.

In general, the TIN surface from a full triangulation "interpolates" the point cloud, that is, it passes through every one of its points. Exceptions occur if there are different data points with the same footprints, that is, duplicate points as mentioned at the beginning of this chapter. In that case, only one of these points can be selected as a vertex of a TIN surface, and it is not possible to pass a TIN surface through all points of the point cloud.

The TIN surface from a partial triangulation provides approximation only, that is, many points of the point cloud are not part of the TIN surface. The quality of the approximation can sometimes be checked by means of visualization. In general, however, there is a need for a numerical

"measure-of-fit,"

that is, a single number "grading" the quality of an approximation. For a point $P_i = (x_i , y_i , z)$ in the point cloud, let $\hat{z}$ denote the elevation of the approximating TIN surface at the footprint $p_i = (x_i , y_i)$ . The

"residual" $r_i = z_i - \hat{z}$

then measures the deviation in the $z$-direction of the data point $P_i$ from the TIN surface. The

"Root-Mean-Square (RMS)": $\sqrt{\frac{1}{n}\sum r_i^2}$

and the

"Average-size-deviation (ASD)": $\frac{1}{n}\sum | r_i |$

of the residuals are the most commonly used measures-of-fit for approximation by an elevated surface. They will be used in this work, too.

## 2.4 THE INSERTION METHOD FOR DELAUNAY TINS

The method implemented in this work for constructing TIN surfaces is based on the so-called

"insertion method"

(Lawson [1977]) in that it sequentially inserts data points as vertices, constructing an intermediate TIN surface each time a new vertex has been added. Thus each additional vertex triggers the update of a previously constructed TIN surface. The process terminates when a specified number of vertices has been reached. After terminating the insertion procedure, it will often be desired to further adjust the resulting TIN surface. Such adjustments are described in Chapter 3.

As a first step, all data footprints are enclosed in a rectangular

$$\text{“map”} \ \{(x,y): \quad x_{\min} \le x \le x_{\max}, \quad y_{\min} \le y \le y_{\max}\},$$

and after including its four corners, the entire map will be covered by the triangulation. If there are no data points at those corners, arbitrary “no data values” will be assigned.

After specifying the map, and possibly cropping to it, the insertion method is applied in two phases. The first phase of the procedure is to construct an

“initial Delaunay triangulation”.

The second phase terminates with the

“specified Delaunay triangulation”,

which now has the specified number of vertices. This triangulation should not be confused with the full triangulation, which includes all possible vertices. During that second phase, each vertex to be inserted next is selected according to an optimization criterion taking into account the current shape of the respective TIN surface.

The simplest way of specifying an initial triangulation is to split the map into two triangles along one of its diagonals. This triangulation is a Delaunay triangulation, which theoretically could serve as an initial triangulation for the second phase. In practice, however, a richer triangulation is recommended for two reasons:

- the NIST method for selecting the vertices to be inserted in phase two is slow if it starts with a small portion of the triangles
- the quality of the vertex selection depends on how well the intermediate TIN surface approximates the point cloud

The NIST meshing procedure uses the insertion method also for phase one, starting with splitting the map into two triangles. Thus the insertion method is used in both phases, the only difference being that during the second phase the vertices are selected for insertion using an adaptive optimization criterion (Section 2.4.1) based on the current surface, whereas during the first phase the insertion sequence is determined independently. In particular, NIST uses the following procedure for constructing the initial Delaunay triangulation:

**Initial Binning:** *Divide the map into an almost square grid of bins. In each bin of the grid select the data point* $P_i$ *whose footprint* $p_i = (x_i, y_i)$ *lies closest to the center of the bin and interpolate this subset of data points by a Delaunay surface.*

Unless empty, each bin contributes a vertex to the initial Delaunay triangulation, and these vertices are inserted by column, first, and by row, second. When using the *TINvolume* routine, the bin size is set by specifying the number of bins per row. The number of bins per column is then automatically chosen so as to make the individual bins as square as possible. The choice of the bin size reflects a balance between two opposite effects: a small bin size leads to a dense initial triangulation and reduces the role of the adaptive vertex selection during the second phase. On the other hand, a large bin size leads to a sparse initial triangulation, increases the role of the second phase, and also tends to increase the overall computational effort. Of course, if a full triangulation is to be determined, the choice of the initial transformation will, in general, not matter.

### 2.4.1 Vertex Selection for Approximation

Phase two of the meshing process applies only to the task of approximation, since for interpolation all data points are considered, and selection of a sample of the data points as vertices of a TIN surface is, therefore, moot. Vertex selection is typically connected with partial triangulation. NIST routines offer two selection criteria. As the next vertex to be inserted, select the data point whose

- vertical distance from the current TIN surface (= size of "residual") is maximum
- product of the vertical distance with the area of the triangle in which its footprint is contained is maximum.

The second option leads to triangulations with more homogeneous triangle size and appears better suited for volume computation. It is, therefore, exclusively used in this work.

### 2.4.2 Inserting a Vertex

The basic procedure is the insertion of a vertex $P_i = (x_i , y_i , z_i)$ into a current TIN surface or, equivalently, the insertion of a footprint $p_i = (x_i , y_i)$ into the underlying triangulation, proceeding as follows. A triangle $t_k$ containing $p_i$ is determined. Exceptional cases aside, $p_i$ lies in the interior of this triangle $t_k$, a new triangulation is then created by connecting $p_i$ to the corners of $t_k$, so that there are now three triangles where previously was just triangle $t_k$. The new triangulation will, in general, no longer be Delaunay, and has to be adjusted. Each adjustment step is an interchange of diagonals in a quadrangle composed of two triangles with a common edge (Fig. 2.4). For details, consult [Witzgall et al., 2004].

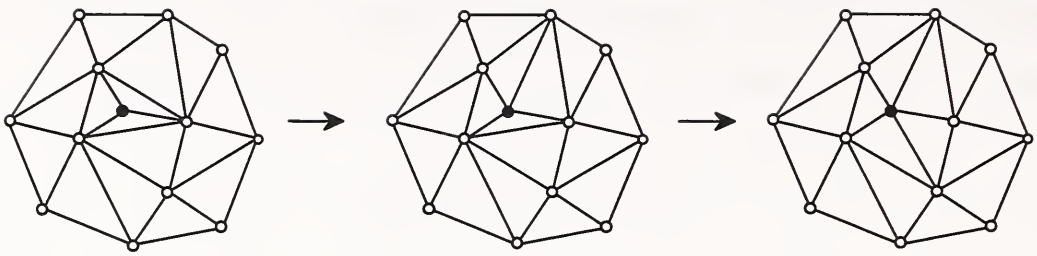

Figure 2.4. Adjustment to achieve a Delaunay triangulation.

# 3. POST-PROCESSING PROCEDURES

In general, once the insertion procedure has been completed, the resulting

"complete triangulation"

requires further editing and adjustment. Such procedures, in particular, the adjustments of vertex elevations and changes in the triangulation are discussed in this chapter. Note that these two adjustments apply only to partial triangulations since these adjustments rely on information provided also by data points which have not been included in the TIN. Filtering and screening options, also described in the chapter, are generally based on full triangulations.

## 3.1 RELEVANT TRIANGLES

The complete triangulation covers the entire map, including "no data" areas of the point cloud such as occlusions or shadows cast by objects in the path of the scan. Among its vertices, the complete triangulation will also contain artificial points such as map corners. In many applications, triangles which contain such artificial vertices or which cover no data areas need to be identified, so that a meaningful

"footprint region"

may be delineated. The approach taken here is to distinguish

"relevant triangles"

among the footprint triangles $t_k$ of the TIN. All other triangles are then removed by marking them a irrelevant, leaving the set of relevant triangles as an instance of a footprint region.

In general, triangles connected to map corners are not relevant. Also, triangles which cover shadows are typically characterized by very long edges or, alternatively, by circumcircles of large diameters. The following choices are therefore offered for designating relevant triangles or, equivalently, deleting irrelevant ones:

- all triangles are relevant, including those with artificial vertices such as map corners
- only triangles meeting map corners and other artificial points are removed
- triangles meeting artificial points or with edges longer than a specified length are removed
- triangles meeting artificial points or with circumcircles larger than a specified diameter are removed. This option relates to the concept of "$\alpha$ -shapes" [Edelsbrunner, Kirkpatrick, and Seidel 1983].

The relevant triangles determine an area of relevance for a given point cloud. Typically, however, the boundary of such an area tends to be very irregular. Options for boundary editing are described in [Witzgall et al. 2004].

## 3.2 ELEVATION ADJUSTMENT

Once a partial triangulation has been completed and its footprint region delineated, it may be desired to improve the RMS measure-of-fit of the approximation of the given point cloud by the corresponding TIN surface. This is done by adjusting vertex elevations while keeping the triangulation fixed. This procedure -- which was examined in all experiments reported here -- is referred to as

"RMS elevation adjustment."

(An ASD elevation adjustment is under development). It is important to realize that it is the approximating TIN surface and not the underlying point cloud that is adjusted by changing the elevations at the vertices of the TIN surface. Any original data point, which was originally selected as a vertex of the TIN surface, remains a member of the point cloud with its given elevation unchanged, regardless of subsequent adjustments to the surface. It thus contributes, like any other data point, to the calculation of the measure-of-fit upon which the approximation is based.

The RMS adjustment amounts to solving a standard "least squares problem" for which many highly developed algorithms are available. The current implementation relies on the following simple iterative scheme. Note that a change of elevation at a vertex $v$ of the TIN surface affects the surface only above the area formed by the triangles adjacent to vertex $v$. This suggests adjusting the elevation at this vertex so that the resulting surface change minimizes the RMS above that area. Carrying out such adjustments in turn for every vertex constitutes an iteration step. For infinitely many steps, the vertex elevations will converge to limits which define the unique "best" TIN surface over the given fixed triangulation and with respect to the RMS norm of vertical residuals. For practical purposes, the process is terminated after (i) a preset number of iterations have been reached, or (*ii*) all individual elevation adjustments during an iteration step have remained below a specified tolerance.

## 3.3 TRIANGULATION ADJUSTMENT

There are situations in which deviations from the Delaunay principle may be called for. This occurs, for instance, if – in terrain parlance – an edge of a Delaunay triangle crosses a valley or tunnels through a ridge (Fig. 3.1). Such situations can be detected if there are sufficiently many data points in the region of the affected triangles. For such cases, the following

"ASD triangulation adjustment"

procedure for adjusting the triangulation has been developed. (The analogous RMS triangulation adjustment has not yet been considred.)

Whenever a strictly convex quadrangle consisting of two adjacent triangles is encountered, it can be checked, whether interchanging the diagonals (Fig. 3.1) improves the ASD measure-of-fit within the quadrangle. The sequence in which the adjustments are carried out matters. In the NIST implementation, the diagonal interchanges with the biggest improvements are carried out first.

The triangle adjustment option was included in Experiment 2 reported below.

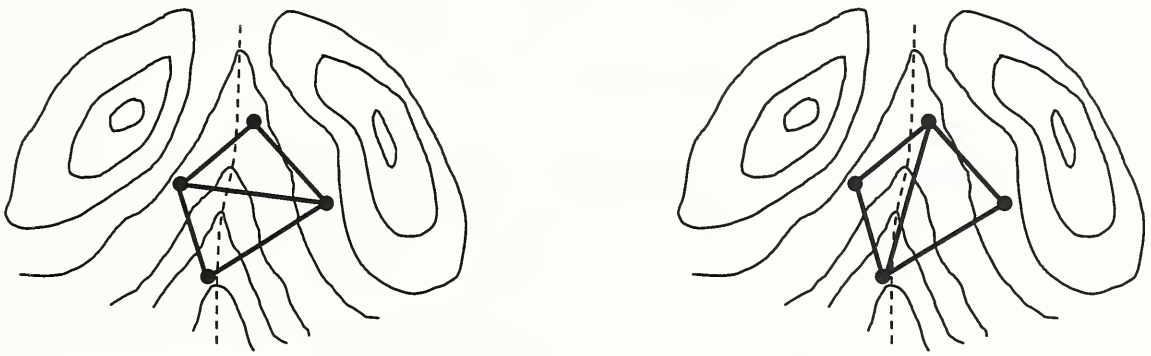

a. Does not retain valley line

b. Retains valley line

Figure 3.1. Adjusting triangles crossing valley.

## 3.4 FILTERING AND SCREENING

TIN methods are also useful for data editing such as removal of "outliers", that is, data points whose elevations drastically exceed the elevation of neighboring data points. In order to achieve such a removal, "filtering" and "screening" methods have been implemented at NIST. In any such method, the elevation $z_i$ of a data point $P_i = (x_i , y_i , z_i)$ is compared to the median of the neighboring data elevations, that is, to the elevations of data points whose footprints are connected to the footprint $p_i = (x_i , y_i)$ of data point $P_i$ by an edge in a TIN triangulation. Typically, full triangulations are used for that purpose. An outlier is then identified as a data point whose elevation differs from the median of the neighboring elevations by more than a specified tolerance.

A screening method, as exemplified by the NIST routine, *TINscreen* , simply deletes outliers from the point cloud. The NIST routine, *TINfilter*, on the other hand, adjusts the elevation of the outlier by replacing it with the value of the median. These routines represent instances of what is usually referred to as a "median filter".

*TINfilter* has been used as an option in Experiment 3 to be reported in Chapter 5.

# 4. CALCULATING VOLUMES

Given the elevation level $z_0$, consider the spatial region bounded below by $z_0$, bounded above by an elevated surface, and bounded either laterally by vertical walls along the boundary of the footprint region or at the intersection of the surface with the elevation level (Fig. 4.1). The volume of that spatial region is called the

"cut volume" $V_{cut}(z_0)$

for the elevation level $z_0$. The corresponding

"fill volume" $V_{fill}(z_i)$

is defined as the volume of the region bounded above by the elevation level $z_0$, and bounded below by the surface. Lateral cut-off is again vertically either along the boundary of the footprint region or at the intersection of surface and elevation level. The projections of the cut and fill volumes ioto the $x,y$-plane cover precisely the footprint area, and meet only along the projections of the lines along which the surface intersects the elevation level. The following discussion is restricted to cut volumes since everything is analogous for fill volumes.

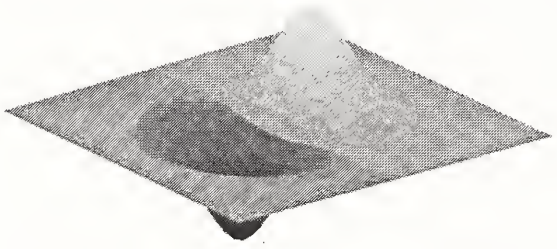

a. Original surface

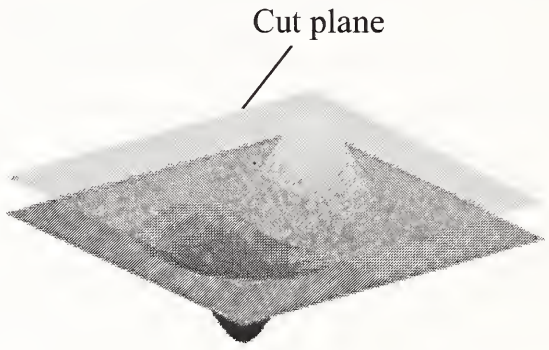


b. Original surface and cut plane

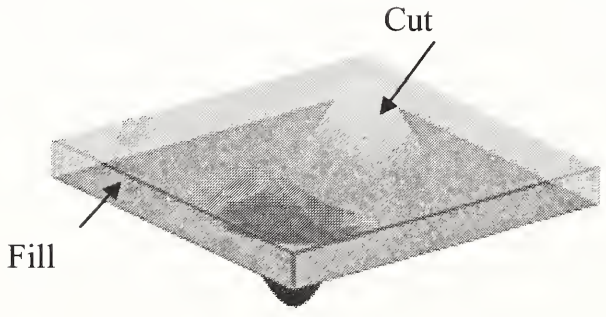


c. Cut volume = volume bounded above by original surface and below by cut plane
Fill volume = volume bounded above by cut plane and below by original surface

Figure 4.1 Schematic illustration of cut and fill volumes.

## 4.1 DECOMPOSITION INTO TRIANGULAR PRISMOIDS

The cut volume $V_{cut}(z_0)$ is readily computed if the bounding elevated surface is a TIN surface. For in this case, the enclosed space is the union of triangular prismoids. As shown in Fig. 4.2,

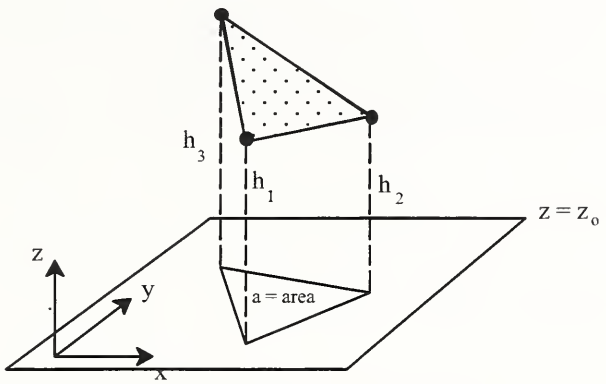


Figure 4.2. A triangular prismoid.

such a "prismoid" is spanned by a usually tilted triangle on top and its footprint at elevation $z_0$ on the bottom. It is bounded at three sides by trapezoids spanned by edges of the top triangle and their respective footprints below. Let

$$h_1, h_2, h_3,$$

denote the lengths of the lateral edges of the trapezoids, that is, the elevations of the top vertices

$$P_{i_1}, P_{i_2}, P_{i_3}$$

above $z_0$. Let also

$A_{foot}$ = area of the footprint triangle,

$V_{prism}$ = volume of the prism.

Then the volume of the prismoid is given by

$$V_{prism} = \frac{h_1 + h_2 + h_3}{3} \times A_{foot}.$$

The decomposition of the volume into triangular prismoids is readily identified. The straight-forward case is that of a surface triangle

$$T_k = (P_{i_1}, P_{i_2}, P_{i_3})$$

with vertices

$$P_{i_1} = (x_{i_1}, y_{i_1}, z_{i_1}), \quad P_{i_2} = (x_{i_2}, y_{i_2}, z_{i_2}), \quad P_{i_3} = (x_{i_3}, y_{i_3}, z_{i_3}).$$

fully above the stipulated elevation level $z_0$. In this case, the triangle $T_k$ by itself, together with its footprint triangle

$$t_k = (p_{i_1}, p_{i_2}, p_{i_3}),$$

with

$$p_{i_1} = (x_{i_1}, y_{i_1}), \quad p_{i_2} = (x_{i_2}, y_{i_2}), \quad p_{i_3} = (x_{i_3}, y_{i_3})$$

defines one of those prismoids, where

$$h_1 = z_{i_1} - z_0 \geq 0, \quad h_2 = z_{i_2} - z_0 \geq 0, \quad h_3 = z_{i_3} - z_0 \geq 0.$$

Should a triangle $T_k$ lie completely below the stipulated elevation level $z_0$, then it does not contribute a prismoid.

There are, however, two intermediate cases as shown in Fig. 4.3. In the first case (Fig. 4.3a), two vertices of triangle $T_k$ lie strictly above the elevation level $z_0$, whereas the remaining vertex lies strictly below. In the second case (Fig. 4.3 b), one vertex lies strictly above, another vertex lies strictly below, with the third one at or below the elevation level $z_0$.

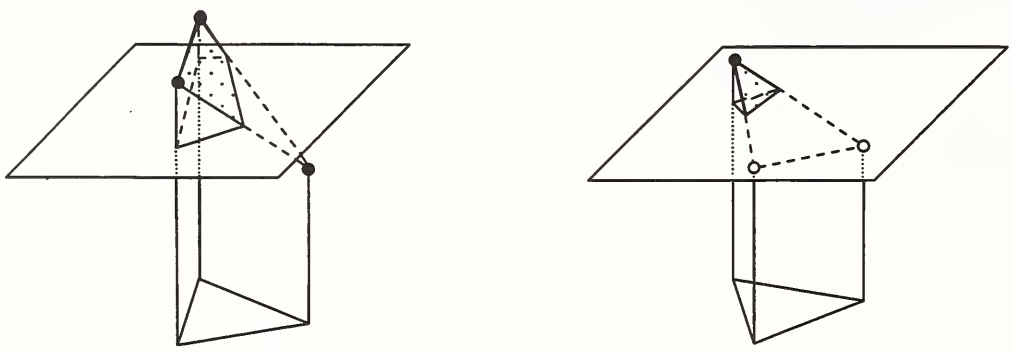

a. b.

Figure 4.3. The triangular prismoid on the right has exactly one vertex above the plane. The one on the left has two.

In both cases, two edges of the triangle $T_k$ intersect the level plane at points

$$p' \text{ and } p'',$$

respectively.

In the first case, only a portion forming a quadrangular prismoid over a quadrangular footprint, say

$$(p_{i_1}, p_{i_2}, p', p'')$$

contributes to the overall volume. Once this footprint quadrangle has been determined, any of its two decompositions into triangles $t'_k$ and $t''_k$, for instance,

$$t'_k = (p_{i_1}, p_{i_2}, p') \text{ and } t''_k = (p_{i_1}, p', p''),$$

will produce two triangular prismoids with the obvious height adjustments.

In the second case, a reduced prismoid results, whose footprint is a triangular portion $t'_k$ of the full footprint of the triangle $T_k$, say

$$t'_k = (p_{i_1}, p', p'').$$

It is obvious that the level volume of a TIN surface depends critically on the definition of the footprint region as discussed in Section 3.1.

## 4.2 FLOOR DETERMINATION

In certain applications, the volume of an object situated on a flat floor is to be found. In this case, it is crucial to determine the elevation of the floor. More generally, there is a need to know when a varying elevation level first meets or leaves an object of interest.

This task is not straightforward because of data noise. The method developed in [Cheok et al., 2000, Witzgall and Cheok, 2001] is to vary the elevation level $z_0$ in equal increments of, say, 1 cm or 0.5 cm, determine cut/fill volumes at these elevations, and then form the first and second differences. As the level plane starts to intersect the portion of the point cloud representing the object, and similarly if the level plane leaves that region, these events are then signaled by a spike in the second differences.

# 5. EXPERIMENTAL VOLUME DETERMINATION

In this chapter, volume determinations from LADAR scans taken inside an NIST building are reported. These determinations are based on two series of LADAR scans of a plywood box, taken from the same instrument location and orientation. The box was built to the following nominal specifications

$$0.9144 \text{ m} \times 1.2192 \text{ m} \times 1.5240 \text{ m} \quad (3 \text{ ft} \times 4 \text{ ft} \times 5 \text{ ft}),$$

and those dimensions were verified to within

$$0.0016 \text{ m} \quad (1/16 \text{ in}).$$

Based on those specifications, a volume of 1.6990 $m^3$ is inferred for the box. It will be convenient, to refer to this value as the "true" volume of the box, realizing full well that this value is still subject to error. Assuming the above error limit of 0.0016 m (1/16 in ) for the linear dimensions of the box, a worst case error estimate places the actual volume between the bounds:

$$1.6990 \text{ m}^3 \pm 0.0059 \text{ m}^3 \text{ or } 1.6990 (1 \pm 0.35 \%) \text{ m}^3 .$$

The LADAR instrument used for the experiment provided coordinate data at the millimeter level, that is, three significant digits after the period if the measurement is reported in meters. A uncertainty of 2 cm or 20 mm is specified by the manufacturer. However, this is the uncertainty for a single measurement which is not the intended function of a LADAR. A LADAR collects millions of points from a scene and these points are then used to generate a surface. This is akin to averaging when the measurements are used, for instance, for the calculations of volumes. As a result, these calculations are more accurate than might be expected in view of the single measurement uncertainty. It was also felt that the standard deviations of the volume results need to be determined without rounding the measurements based on the manufacturer's specifications. For these reasons, three digits after the period, when expressed in meters, were retained, and for the reports of the experiments, the calculated volumes, averages, and standard deviations were reported up to four digits after the period.

In one series of the experimental scans, a free-standing screen of plywood sheets was placed against those two faces of the box that remained obscured when scanned from the instrument location. In a parallel series, the box had been removed so that only the screen remained in its original position (Fig. 1.1). Five different point density settings were used when generating the two series of scans.

Using the same window for cropping the ten original data sets – five scans of the screen by itself and five scans of the screen with the box – the data sets of the following sizes were obtained (Table 5.1).

Table 5.1. Sizes of data files after cropping.

| Density setting | Without Box | | With Box | |
|---|---|---|---|---|
| | Filename | No. of points | Filename | No. of points |
| 1 | PtC_no_bx_1a.dat | 15 903 | PtC_scr_1a.dat | 15 912 |
| 2 | PtC_no_bx_2.dat | 10 221 | PtC_scr_2.dat | 10 199 |
| 3 | PtC_no_bx_3.dat | 7 104 | PtC_scr_3.dat | 7 116 |
| 4 | PtC_no_bx_4.dat | 3 990 | PtC_scr_4.dat | 3 995 |
| 5 | PtC_no_bx_5.dat | 2 548 | PtC_scr_5a.dat | 2 557 |

An uncropped footprint triangulation of the point cloud from scanning the box with screen at the highest density setting is displayed in Fig. 5.1. It displays strips of high density marking the location of the screen and two vertical walls of the box. Indeed, the signal returns from vertical walls will generate data footprints that accumulate the "base" of those walls. Because of the higher angle of incidence, data density is higher on the floor than on top of the box. In Fig. 5.1, the effects of beam spread can be observed at the bottom portion of the screen to the left. Such "phantom points" and "mixed pixels" are a well recognized phenomenon capable of introducing errors in surface modeling.

To exclude signal returns beyond the location of the screens, all ten point clouds were cropped along the left screen in Fig. 5.1 as indicated in Fig. 5.2.

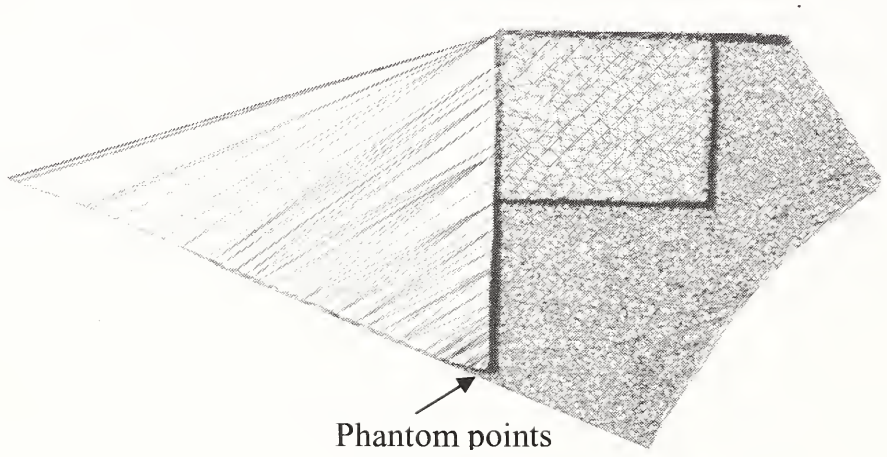


Figure 5.1. Triangulation of uncropped data sets.

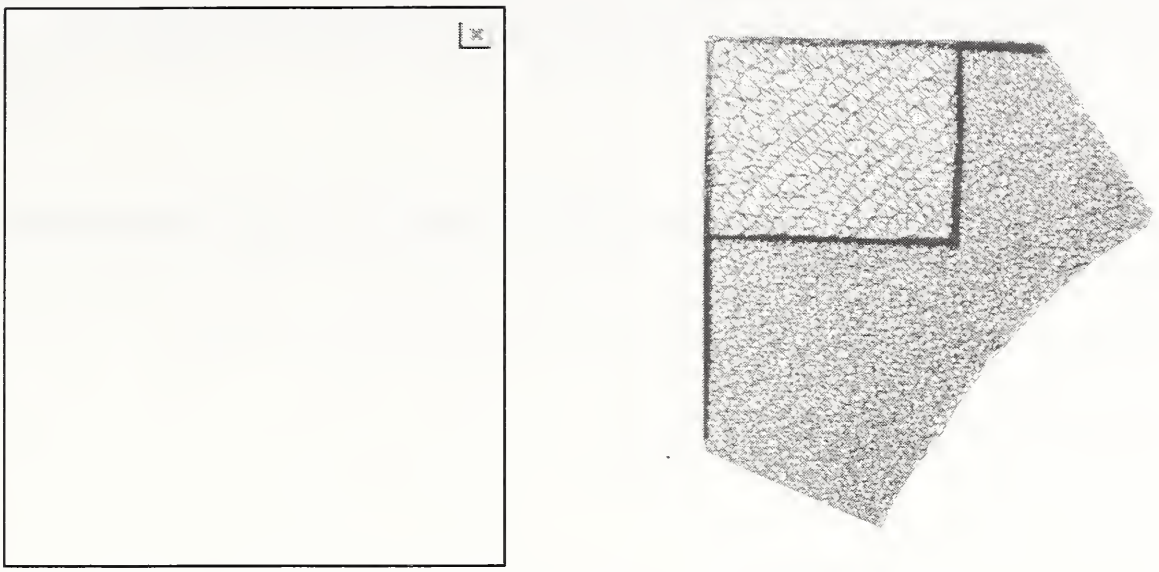

Figure 5.2. Cropped data sets displayed as footprint triangulations.

In each experiment, a pair of point clouds arising from corresponding scans with and without the box, respectively, was meshed as part of the volume calculation. Then the volumes above a common horizontal, below-the-floor, level were calculated for each of the two resulting TIN surfaces. The difference between those two separate volume measurements should then account for the volume of the box.

As described in Chapter 4, volume calculations are geared to specified elevation levels characterized by specified values of the coordinate $z$ . The cut volumes are, therefore, above the specified $z$-level and below the given TIN surface, fill volumes are below the specified $z$-level and above the given TIN surface. The volume routine repeatedly prompts for specific $z$-levels for which it then provides both cut and fill volumes. In the first three experiments described below, any two volumes, whose difference is taken as the volume of the box, are cut volumes with respect to the same $z$-level, which is chosen sufficiently low to yield a fill volume of zero.

Suppose two elevation levels $z_1$ and $z_2 > z_1$ are such that the fill volume at these levels vanishes. Then the difference between the corresponding cut volumes $V_{cut}(z_1) > V_{cut}(z_2)$ is given by the area of the footprint region of the TIN surface multiplied by the difference in those elevation levels:

$$V_{cut}(z_1) - V_{cut}(z_2) = area_{\text{footprint}} \times (z_2 - z_1).$$

In the case of TIN surfaces representing the screen by itself and the screen with the box, the footprint areas differ slightly. There is therefore a slight dependence of the volume difference on the choice of a common $z$-level with zero fill volume. In view of this dependence, the common $z$-level was generally chosen as high as possible while the fill volume remained at zero. In one of two methods used in Experiment 4, a different approach was taken. Here the volume difference

was formed from fill volumes as the $z$-levels were reduced, moving away from the instrument, as described below, slightly different $z$-levels were determined for the two fill volumes.

## 5.1 EXPERIMENT 1

In this experiment, only the pair of scans of the highest density setting has been considered. As explained in the previous sections, the meshing process employed here offers various options and requires choices of several process parameters. The first experiment to be described here aims to explore the sensitivity of the volume calculations with respect to two parameters,

- bin size for pre-binning (Section 2.4),
- number of vertices in the final triangulation,

and to the option of choosing

- RMS elevation adjustments (Section 3.2).

The results of Experiment 1 are listed in Table 5.2 and graphically displayed in Fig. 5.3.

The bin size chosen for the pre-binning mechanism determines the set of data points entering the initial triangulation and, therefore, its size and shape. Since a data point is chosen from each non-empty bin, small bin size or, equivalently, a large number of bins per row, leads to a dense initial triangulation. In this case, a smaller percentage of the specified number of vertices is chosen adaptively, that is, based on the respective state of the surface. Conversely, few bins per row result in a sparse initial triangulation, and a larger portion of the vertices chosen adaptively. In the following Table 5.2, entries for large numbers of bins – resulting in small individual bin sizes – cannot be obtained if they exceed the specified number of vertices. This is because selecting a vertex in each non-empty bin for an initial triangulation may already exceed the specified limit. In this experiment, the volume computations do not appear very sensitive to variations in bin size and the resulting perturbations of the TIN triangulation.

The number of data points to be selected as vertices of the TIN surface is a more significant parameter than the bin size. The reader might be under the impression that not using a full triangulation would be tantamount to ignoring a part of the scan information. It should be kept in mind, however, that to restrict the number of vertices of the TIN surface is not to restrict the number of data points considered. In effect, the number of vertices specified for the TIN surface defines the resolution of the mesh which represents the point cloud. During the adaptive vertex selection process every data point plays a role in that selection. The full data information is therefore already reflected in the shape of any TIN surface which has been based on an adaptively selected vertex sample. Finally, error statistics are based on the full data sets. For these reasons, information from data points not included as vertices in the TIN is indeed utilized.

An unexpected trend was observed: as the specified number of vertices increases, the resulting volume estimates decrease. It is not yet known whether this trend represents a general phenomenon. The data set also provides an example where the highest surface resolution, as

defined by the number of vertices and, consequently, triangles, does not yield the most accurate result. That result is achieved when the number of vertices is approximately 1/3 of the number of data points. This may well be a general phenomenon, although much more evidence needs to be collected.

The RMS elevation adjustment does not appear to improve the results significantly. Since the adjustment is based mainly on those data points which have not been selected as vertices, its effect will be progressively diminished as there are fewer such data points.

In subsequent experiments, volume calculations will be based on the vertex ratio of 1/3, although there is little evidence as whether this parameter choice is optimal. Assuming this vertex ratio, this translates into specifying 5000 vertices for the TIN surfaces to be used for volume calculation for this experiment. The volumes reported in Table 5.2 for the corresponding six bin size specifications range from 1.6974 $m^3$ to 1.7021 $m^3$ with mid point 1.69975 $m^3$ with RMS adjustment, and from 1.7029 $m^3$ to 1.6986 $m^3$ with midpoint 1.70075 $m^3$ without RMS adjustment. The following volume result may thus be associated with Experiment 1 and compared to the "true" value of 1.6990 $m^3$ :

$$1.6997\ m^3 \pm 0.00235\ m^3 \quad \text{(with RMS adjustment)}$$
$$1.7007\ m^3 \pm 0.00215\ m^3 \quad \text{(without RMS adjustment)}$$

The uncertainties based on the observed range of values for 5000 vertices are thus on the order of 0.14 % and 0.13 % , respectively.

Table 5.2. Results of Experiment 1.

| # Points In Mesh | %[a] of Total Pts. | Volume ($m^3$) | | | | | | | % Error in Volume | | | | | | |
|---|---|---|---|---|---|---|---|---|---|---|---|---|---|---|---|
| | | 15 bin | 20 bin | 25 bin | 30 bin | 40 bin | 100 bin | 200 bin | 15 bin | 20 bin | 25 bin | 30 bin | 40 bin | 100 bin | 200 bin |
| | | With RMS Adjustment | | | | | | | With RMS Adjustment | | | | | | |
| 3K, rms | 19 | 1.7044 | 1.7043 | 1.7055 | 1.7015 | 1.7035 | | | 0.3178 | 0.3119 | 0.3826 | 0.1471 | 0.2649 | | |
| 4K, rms | 25 | 1.7026 | 1.7007 | 1.7010 | 1.6988 | 1.7013 | | | 0.2119 | 0.1001 | 0.1177 | -0.0118 | 0.1354 | | |
| 5K, rms | 31 | 1.7021 | 1.6998 | 1.7008 | 1.7002 | 1.6995 | 1.6974 | | 0.1825 | 0.0471 | 0.1059 | 0.0706 | 0.0294 | -0.0942 | |
| 6K, rms | 37 | 1.7003 | 1.6982 | 1.6982 | 1.6980 | 1.6980 | 1.7002 | | 0.0765 | -0.0471 | -0.0471 | -0.0589 | -0.0589 | 0.0706 | |
| 7K, rms | 44 | 1.6975 | 1.6976 | 1.6967 | 1.6971 | 1.6966 | 1.6955 | | -0.0883 | -0.0824 | -0.1354 | -0.1118 | -0.1413 | -0.2060 | |
| 8K, rms | 50 | 1.6968 | 1.6973 | 1.6961 | 1.6964 | 1.6965 | 1.6961 | 1.6947 | -0.1295 | -0.1001 | -0.1707 | -0.1530 | -0.1471 | -0.1707 | -0.2531 |
| 9K, rms | 56 | 1.6974 | 1.6977 | 1.6962 | 1.6974 | 1.6964 | 1.6952 | 1.6957 | -0.0942 | -0.0765 | -0.1648 | -0.0942 | -0.1530 | -0.2237 | -0.1942 |
| 10K, rms | 62 | 1.6960 | 1.6964 | 1.6962 | 1.6971 | 1.6962 | 1.6954 | 1.6952 | -0.1766 | -0.1530 | -0.1648 | -0.1118 | -0.1648 | -0.2119 | -0.2237 |
| 13K, rms | 81 | 1.6949 | 1.6949 | 1.6945 | 1.6949 | 1.6948 | 1.6950 | 1.6945 | -0.2413 | -0.2413 | -0.2649 | -0.2413 | -0.2472 | -0.2354 | -0.2649 |
| 16K, rms | 100 | 1.6946 | 1.6947 | 1.6945 | 1.6946 | 1.6946 | 1.6946 | 1.6945 | -0.2590 | -0.2531 | -0.2649 | -0.2590 | -0.2590 | -0.2590 | -0.2649 |
| | | Without RMS Adjustment | | | | | | | Without RMS Adjustment | | | | | | |
| 3K | 19 | 1.7058 | 1.7059 | 1.7046 | 1.7021 | 1.7019 | | | 0.4002 | 0.4061 | 0.3296 | 0.1825 | 0.1707 | | |
| 4K | 25 | 1.7024 | 1.7022 | 1.7004 | 1.7023 | 1.6999 | | | 0.2001 | 0.1883 | 0.0824 | 0.1942 | 0.0530 | | |
| 5K | 31 | 1.7029 | 1.6986 | 1.7005 | 1.7015 | 1.6993 | 1.6988 | | 0.2295 | -0.0235 | 0.0883 | 0.1471 | 0.0177 | -0.0118 | |
| 6K | 37 | 1.7007 | 1.6973 | 1.6982 | 1.6980 | 1.6976 | 1.7007 | | 0.1001 | -0.1001 | -0.0471 | -0.0589 | -0.0824 | 0.1001 | |
| 7K | 44 | 1.6984 | 1.6977 | 1.6973 | 1.6975 | 1.6958 | 1.6970 | | -0.0353 | -0.0765 | -0.1001 | -0.0883 | -0.1883 | -0.1177 | |
| 8K | 50 | 1.6964 | 1.6956 | 1.6954 | 1.6958 | 1.6949 | 1.6953 | 1.6939 | -0.1530 | -0.2001 | -0.2119 | -0.1883 | -0.2413 | -0.2178 | -0.3002 |
| 9K | 56 | 1.6971 | 1.6968 | 1.6961 | 1.6971 | 1.6955 | 1.6948 | 1.6954 | -0.1118 | -0.1295 | -0.1707 | -0.1118 | -0.2060 | -0.2472 | -0.2119 |
| 10K | 62 | 1.6953 | 1.6953 | 1.6957 | 1.6967 | 1.6949 | 1.6948 | 1.6950 | -0.2178 | -0.2178 | -0.1942 | -0.1354 | -0.2413 | -0.2472 | -0.2354 |
| 13K | 81 | 1.6944 | 1.6941 | 1.6941 | 1.6947 | 1.6935 | 1.6942 | 1.6936 | -0.2707 | -0.2884 | -0.2884 | -0.2531 | -0.3237 | -0.2825 | -0.3178 |
| 16K | 100 | 1.6941 | 1.6939 | 1.6941 | 1.6944 | 1.6935 | 1.6939 | 1.6937 | -0.2884 | -0.3002 | -0.2884 | -0.2707 | -0.3237 | -0.3002 | -0.3119 |

a. Rounded to nearest integer

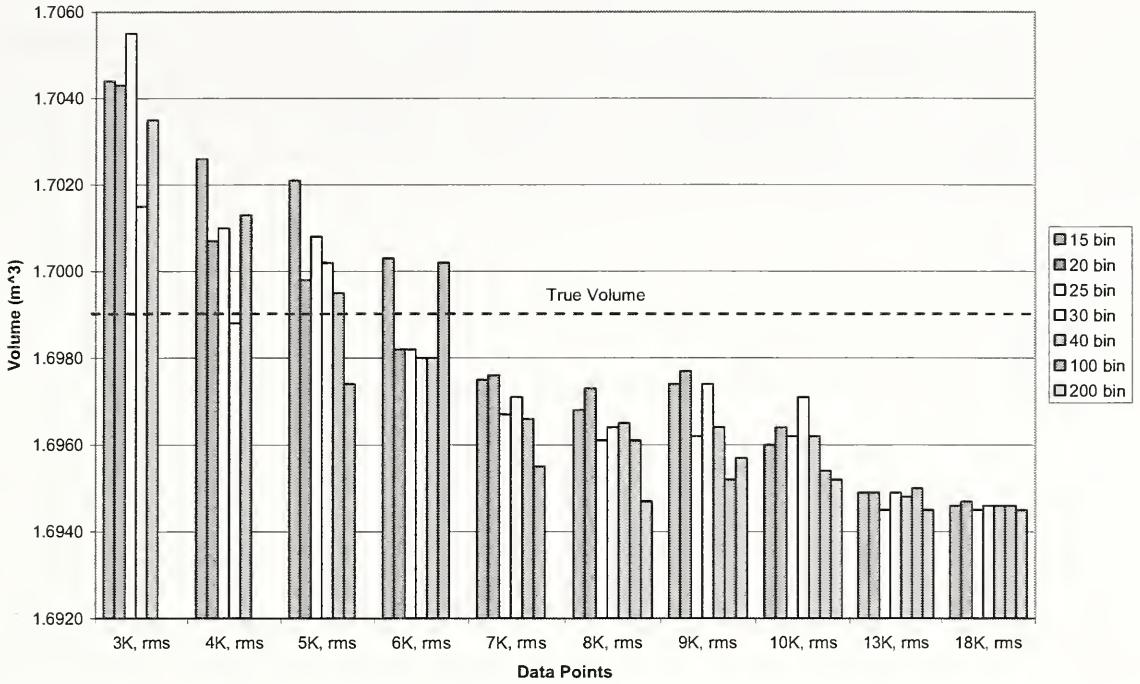


a. With RMS Adjustment

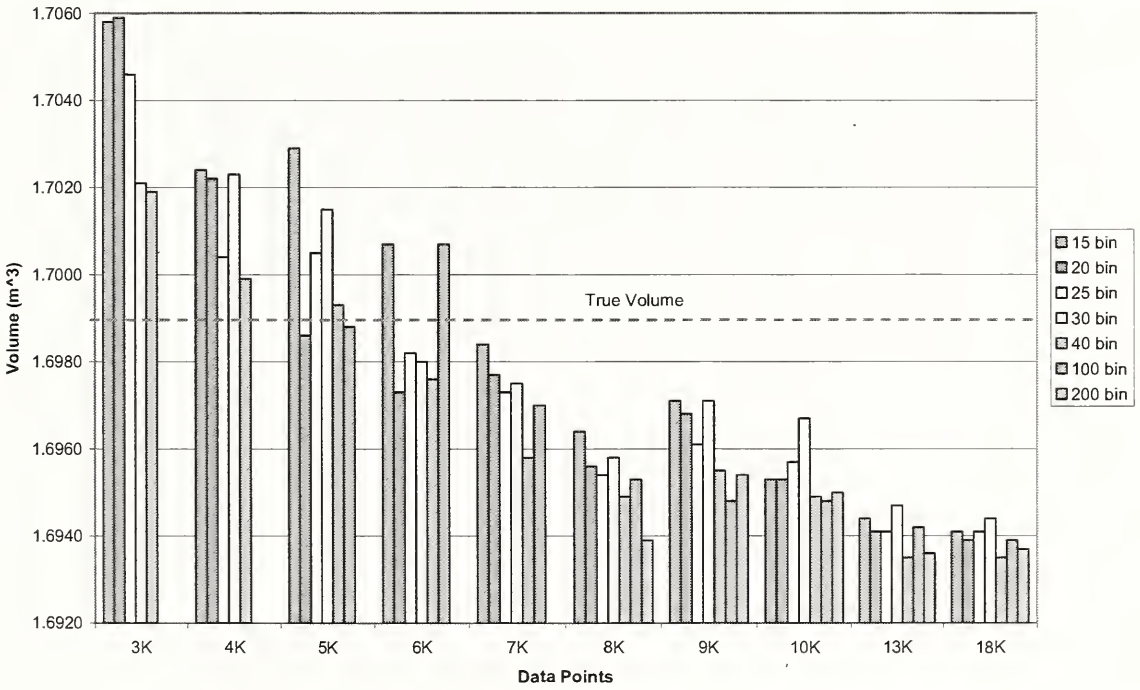


b. Without RMS Adjustment

Figure 5.3. Plot of volume vs. number of points in sub-sample and number of bins. (a)With and (b)Without RMS Adjustment.

## 5.2 EXPERIMENT 2

In this experiment all five pairs of scans – each pair taken with different point densities – were analyzed. TIN surfaces were constructed by adaptively selecting approximately 1/3 of the data points as vertices. For each density, the volumes associated with these TIN surfaces are calculated in four different ways, depending on whether elevation adjustment (Section 3.2) and or triangulation adjustment (Section 3.3) are employed:

- No adjustment
- RMS elevation adjustment only
- Triangulation adjustment
- RMS elevation adjustment followed by triangulation adjustment

A volume was also calculated using all points of the point cloud from the lowest density setting. For such full triangulations, adjustments are not applicable since there are essentially no data points available for adjustments as essentially all the points are incorporated as vertices into the respective surfaces. The volume errors are plotted (Fig. 5.4) and tabulated (Table 5.3a). It is not understood why the experimental volumes consistently underestimate the "true" value. Even more puzzling is the fact that the errors don't consistently increase with decreasing data density.

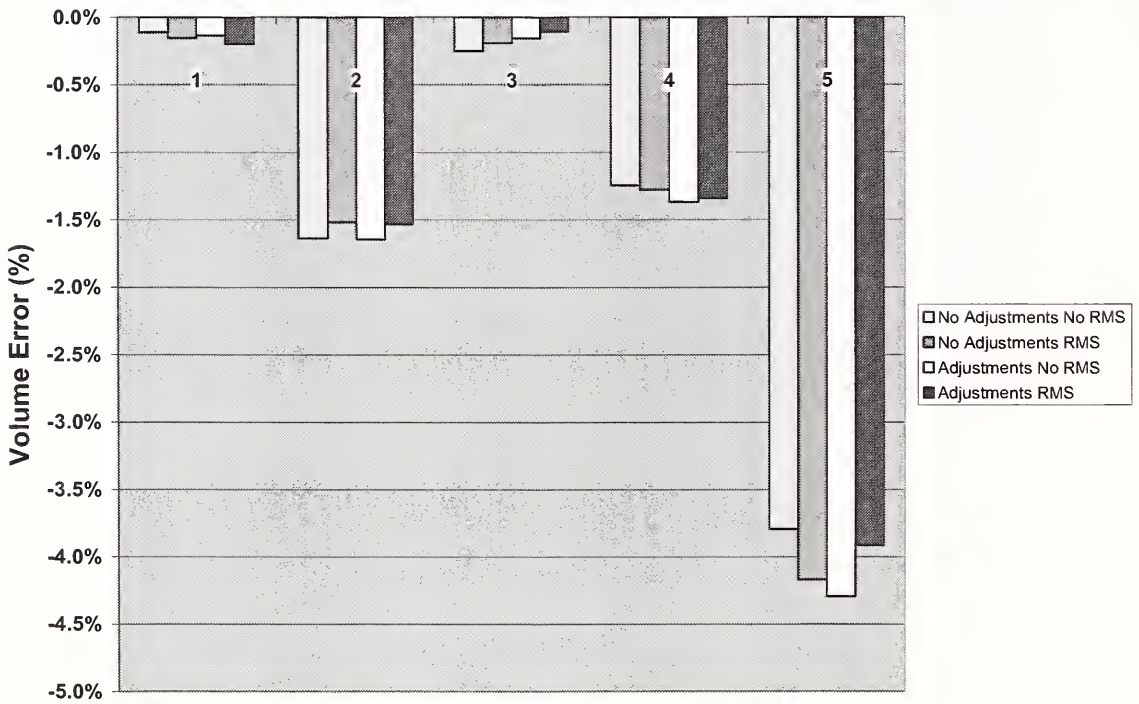


Figure 5.4. Experiment 2: Error plot for volumes for scan sets 1 to 5.

Table 5.3a. Experiment 2: Volume Errors

| Filename | #pts in orig. file | #pts. used in mesh | % of total points | Volume Error (%) | | | |
|---|---|---|---|---|---|---|---|
| | | | | No Triangulation Adjustments | | Triangulation Adjustments | |
| | | | | No RMS | RMS | No RMS | RMS |
| PtC_scr_1a.dat / PtC_no_bx_1a.dat | 15912 / 15903 | 5000 / 5000 | 31 | -0.11 | -0.15 | -0.14 | -0.20 |
| PtC_scr_2.dat / PtC_no_bx_2.dat | 10199 / 10221 | 3500 / 3500 | 34 | -1.64 | -1.52 | -1.64 | -1.53 |
| PtC_scr_3.dat / PtC_no_bx_3.dat | 7116 / 7104 | 2500 / 2500 | 35 | -0.25 | -0.19 | -0.16 | -0.11 |
| PtC_scr_4.dat / PtC_no_bx_4.dat | 3995 / 3990 | 1500 / 1500 | 38 | -1.25 | -1.28 | -1.37 | -1.34 |
| PtC_scr_5a.dat / PtC_no_bx_5.dat | 2557 / 2548 | 800 / 800 | 31 | -3.79 | -4.17 | -4.29 | -3.91 |
| PtC_scr_5a.dat / PtC_no_bx_5.dat | 2557 / 2548 | 2557 / 2548 | 100 | -4.97 | N/A | N/A | N/A |

Table 5.3b. Experiment 2: ASD and RMS Errors

| Filename | ASD Errors (cm) | | | | RMS Errors (cm) | | | |
|---|---|---|---|---|---|---|---|---|
| | No Triangulation Adjustments | | Triangulation Adjustments | | No Triangulation Adjustments | | Triangulation Adjustments | |
| | No RMS | RMS | No RMS | RMS | No RMS | RMS | No RMS | RMS |
| PtC_scr_1a.dat | 11.882 | 10.263 | 11.796 | 10.226 | 23.227 | 16.622 | 23.186 | 16.601 |
| PtC_no_bx_1a.dat | 12.146 | 10.544 | 12.041 | 10.512 | 24.187 | 17.319 | 24.139 | 17.301 |
| PtC_scr_2.dat | 10.891 | 9.802 | 10.726 | 9.742 | 21.961 | 16.104 | 21.844 | 16.067 |
| PtC_no_bx_2.dat | 10.578 | 9.642 | 10.374 | 9.554 | 21.842 | 16.118 | 21.674 | 16.056 |
| PtC_scr_3.dat | 10.645 | 9.797 | 10.460 | 9.713 | 21.620 | 16.136 | 21.473 | 16.076 |
| PtC_no_bx_3.dat | 10.537 | 9.730 | 10.201 | 9.588 | 21.873 | 16.143 | 21.551 | 16.045 |
| PtC_scr_4.dat | 10.194 | 9.413 | 9.783 | 9.289 | 20.955 | 15.663 | 20.528 | 15.574 |
| PtC_no_bx_4.dat | 9.780 | 9.124 | 9.358 | 8.948 | 20.588 | 15.307 | 20.134 | 15.161 |
| PtC_scr_5a.dat | 12.158 | 11.002 | 11.532 | 10.859 | 23.503 | 17.488 | 22.854 | 17.384 |
| PtC_no_bx_5.dat | 11.297 | 10.374 | 10.495 | 10.171 | 22.418 | 16.978 | 21.334 | 16.799 |
| PtC_scr_5a.dat[1] | N/A | N/A | N/A | N/A | N/A | N/A | N/A | N/A |
| PtC_no_bx_5.dat[1] | N/A | N/A | N/A | N/A | N/A | N/A | N/A | N/A |

[1] These values are not meaningful when all the data points are used in the mesh.

In addition, RMS and ASD approximation errors are tabulated for each surface pair (Table 5.3b) except for the surface pair arising from a full triangulation. These errors do not refer to the direct accuracy as based on deviations of the generated TIN surfaces from the known surface of the box, but rather to the accuracy based on residual deviations of the data points from the TIN surface derived from a subset of the data points. Table 5.3b shows that increased accuracy of approximation, as measured by either RMS or ASD errors, does not necessarily correlate with increased accuracy of volume calculation, which represents a direct accuracy measurement.

Again, representative values are derived for the five point clouds based on the approximate vertex to data ratio of 1/3. For each density level, the four volume measurements are used to derive the range and the midpoint as shown in Table 5.4.

Table 5.4. Experiment 2: Volumes.

| Density Level | Volume ($m^3$) | | | | Mid-Range Volume ($m^3$) |
|---|---|---|---|---|---|
| 1 | 1.697 | 1.696 | 1.697 | 1.696 | 1.6964 ± 0.00700 |
| 2 | 1.671 | 1.673 | 1.671 | 1.673 | 1.6721 ± 0.00105 |
| 3 | 1.695 | 1.696 | 1.696 | 1.697 | 1.6959 ± 0.00125 |
| 4 | 1.678 | 1.677 | 1.676 | 1.676 | 1.6768 ± 0.00100 |
| 5 | 1.635 | 1.628 | 1.626 | 1.633 | 1.6303 ± 0.00425 |
| 5 - Full set | 1.615 | NA | NA | NA | NA |

Note that the observed volume ranges do not include the "true" value 1.6990 $m^3$. As mentioned before, the reasons for this bias are unknown.

## 5.3 EXPERIMENT 3

This experiment aims at deriving statistical error measures for volume calculation. From each of the two densest scans – screen with and without box – ten reduced files were created by randomly selecting 50 % of the data points, respectively. For each of the ten pairs of data sets, volumes were calculated. This procedure made it possible to determine an expected value and a standard deviation from the ten volumes obtained. All surfaces were constructed with or without employing the median filter *TINfilter* in order to smooth the surface (Section 3.4).

Table 5.5. Volume and statistics for Experiment 3.

| File Number | Volume ($m^3$) | | | |
|---|---|---|---|---|
| | No Filter | | Filter | |
| | w/ RMS adjustment | w/o RMS adjustment | w/ RMS adjustment | w/o RMS adjustment |
| 1 | 1.691 | 1.693 | 1.686 | 1.677 |
| 2 | 1.678 | 1.672 | 1.669 | 1.664 |
| 3 | 1.686 | 1.687 | 1.669 | 1.669 |
| 4 | 1.665 | 1.669 | 1.659 | 1.659 |
| 5 | 1.674 | 1.674 | 1.662 | 1.653 |
| 6 | 1.681 | 1.682 | 1.669 | 1.667 |
| 7 | 1.673 | 1.689 | 1.674 | 1.676 |
| 8 | 1.685 | 1.689 | 1.678 | 1.680 |
| 9 | 1.664 | 1.668 | 1.661 | 1.658 |
| 10 | 1.678 | 1.688 | 1.664 | 1.663 |
| **Average Volume ($m^3$)** | 1.678 | 1.681 | 1.669 | 1.667 |
| **Std. dev. ($m^3$)** | 0.0086 | 0.0094 | 0.0085 | 0.0089 |
| **Volume Error ($m^3$)** | -0.021 | -0.018 | -0.030 | -0.032 |
| **Vol. Error (%)** | **-1.26** | **-1.05** | **-1.79** | **-1.91** |

Note that the directly measured "true" volume of the box differs by more than two standard deviations from the expected value based on the ten volume measurements in Table 5.5. The reasons for that apparent bias remain unclear. As in Experiment 2, the "true" volume is consistently underestimated. Unexpectedly, the underestimation is even larger when the point cloud has been pre-cleaned using the median filter.

## 5.4 EXPERIMENT 4

This experiment also uses the same ten random samples of 50 % of the data from the densest scans as Experiment 3, and calculates volumes for the resulting ten pairs of data sets as well as for the full data set. However, meshing is now carried out in a different coordinate system, where the $z$-axis points in the opposite direction of an estimated general scan direction. The scan direction estimate was obtained from a graphic display of the footprint triangulation. Note that increasing the $z$-level for the volume calculation moves the floor towards the instrument. Cut volumes are oriented towards the instrument, fill volumes away from it.

Two methods for calculating volumes were employed, based on comparing cut and fill volumes, respectively. The first method, "Method 1", determines floor levels that – when applied to the scans with the box – are close to the box but separate it from the instrument. The volume of the box is then recovered as the difference of the fill volume without the box and the fill volume with the box. Fig. 5.5a schematically illustrates this approach in 2D.

a. Method 1

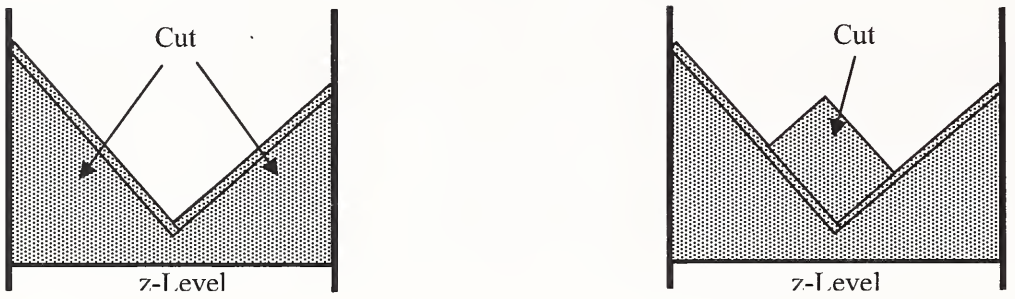


b. Method 2

Figure 5.5. Schematic illustration of two methods for determining the volume of a box.

The second method, Method 2, uses floor levels which are located beyond the scanned objects as viewed from the instrument and indicated by zero fill volumes. The difference of the cut volumes with and without the box is then considered to be the volume of the box. A schematic illustration of this second approach is provided in Fig. 5.5b.

All relevant triangles together define the footprint area of the meshed TIN surface. It was observed that the screen with the box occupies a slightly larger footprint area than the screen without the box (5.446 $m^2$ vs. 5.442 $m^2$). Since the footprint area represents the silhouette of the screen as seen by the instrument, this area should be the same before and after the removal of the box. The discrepancy in the footprint areas may thus suggest that a slight movement of the screen occurred after the box was removed. Another indication is the existence of a shift in the sequence of cut volumes in the region between the box and the instrument. In this region, only the screen contributes to cut volumes, and these cut volumes should therefore agree for identical floor levels unless the scene was perturbed. Table 5.6 shows corresponding portions of the two sequences, where $z$-levels are varied in steps of 0.2 cm between -30 cm and -80 cm. These two sequences will be used to determine an offset between them.

Table 5.6. Cut volume comparison for data with and without box.

| Floor Level (cm) | w/ Box Cut Volume (cm^3) | w/o Box Cut Volume (cm^3) |
|---|---|---|
| -30 | 70 | 53 |
| -30.2 | 80 | 58 |
| -30.4 | 87 | 65 |
| -30.6 | 94 | 73 |
| -30.8 | 105 | 80 |
| -31 | 114 | 89 |
| -31.2 | 124 | 97 |
| -31.4 | 138 | 107 |
| -31.6 | 148 | 116 |
| -31.8 | 159 | 126 |
| -32 | 172 | 139 |
| -32.2 | 187 | 151 |
| -32.4 | 200 | 165 |
| -32.6 | 214 | 175 |
| -32.8 | 231 | 189 |
| -33 | 246 | 205 |
| ⋮ | ⋮ | ⋮ |
| -78.2 | 84954 | 81639 |
| -78.4 | 85906 | 82549 |
| -78.6 | 86872 | 83466 |
| -78.8 | 87845 | 84380 |
| -79 | 88825 | 85300 |
| -79.2 | 89808 | 86230 |
| -79.4 | 90818 | 87162 |
| -79.6 | 91813 | 88096 |
| -79.8 | 92823 | 89043 |
| -80 | 93844 | 89983 |

| Offset (cm) | Sum of Squares of Differences ($cm^3$) |
|---|---|
| 0.4 | 9652.648 |
| 0.6 | 3336.779 |
| 0.8 | 6552.811 |
| 1.0 | 13630.473 |

The two sequences of cut volumes shown in Table 5.6 appear to be offset by 0.6 cm. To verify this, the square roots of the sum of squares of differences was calculated for the four offsets of 0.4 cm, 0.6 cm, 0.8 cm, respectively, and are displayed at the bottom of Table 5.6. They confirm that the offset of 0.6 cm provides a better match than the other three choices in the sense of least squares. That offset needs to be taken into account when cut volumes of the screen with and without box are compared. Thus, in both methods for volume determination as implemented in this work, floor levels that correspond to each other differ by 0.6 cm.

Tables 5.7a and 5.7b present volume results for the full data set, with and without RMS adjustment, respectively. 6 000 points – roughly one third of the data points – were adaptively selected as vertices of the TIN surface. Cut and fill volumes for both the scans with and without the box are listed. These volumes are given for five pairs of corresponding floor levels – in steps

of 5.0 cm – that serve as reference for their computation. Note that for Method 1, the floor level of -74.4 cm for the scan with the box corresponds to the floor level of -75.0 cm for the scan without. These floor levels have been selected so as to be close to the box without intersecting it. Similarly, for Method 2, the floor level of -284.4 cm corresponds to the floor level of -285 cm for the other scan of the pair. These floor levels have been chosen for zero fill volumes. For both methods, the volumes are sensitive to the choice of the reference floor level: the relationship is not noisy, but exhibits a linear trend. The reason for this is unclear. The results of Method 2 appear to be less accurate. This might be due to the fact that the footprint area of the scan without the box is slightly smaller than the footprint area with the box: the cut volume of the scan without the box is thus reduced and, as this value is subtracted to arrive at the volume, the volume is correspondingly increased.

Table 5.7a. Volume computation with RMS adjustments for the full data set.

| Floor Level (cm) | Box –unsampled 6000 points meshed | | Floor Level (cm) | No Box – unsampled 6000 points meshed | | Box Vol. ($m^3$) | Error (%) |
|---|---|---|---|---|---|---|---|
| | Cut Volume ($cm^3$) | Fill Volume ($cm^3$) | | Cut Volume ($cm^3$) | Fill Volume ($cm^3$) | | |
| **Method 1** | | | | | | | |
| -54.4 | N/A | 4280545 | -55 | N/A | 5981733 | 1.7012 | 0.13 |
| -59.4 | N/A | 4017048 | -60 | N/A | 5718737 | 1.7017 | 0.16 |
| -64.4 | N/A | 3756907 | -65 | N/A | 5459025 | 1.7021 | 0.18 |
| -69.4 | N/A | 3500145 | -70 | N/A | 5202554 | 1.7024 | 0.20 |
| -74.4 | N/A | 3246716 | -75 | N/A | 4949387 | 1.7027 | 0.22 |
| **Method 2** | | | | | | | |
| -284.4 | 8257297 | N/A | -285 | 6548046 | N/A | 1.7093 | 0.60 |
| -289.4 | 8529598 | N/A | -290 | 6820171 | N/A | 1.7094 | 0.61 |
| -294.4 | 8801899 | N/A | -295 | 7092297 | N/A | 1.7096 | 0.62 |
| -299.4 | 9074201 | N/A | -300 | 7364422 | N/A | 1.7098 | 0.63 |

Table 5.7b. Volume computation without RMS adjustments for the full data set.

| Floor Level (cm) | Box – unsampled 6000 points meshed | | Floor Level (cm) | No Box – unsampled 6000 points meshed | | Box Vol. ($m^3$) | Error (%) |
|---|---|---|---|---|---|---|---|
| | Cut Volume ($cm^3$) | Fill Volume ($cm^3$) | | Cut Volume ($cm^3$) | Fill Volume ($cm^3$) | | |
| **Method 1** | | | | | | | |
| -54.4 | N/A | 4276612 | -55 | N/A | 5981594 | 1.7050 | 0.35 |
| -59.4 | N/A | 4013304 | -60 | N/A | 5718545 | 1.7052 | 0.37 |
| -64.4 | N/A | 3753258 | -65 | N/A | 5458852 | 1.7056 | 0.39 |
| -69.4 | N/A | 3496743 | -70 | N/A | 5202352 | 1.7056 | 0.39 |
| -74.4 | N/A | 3243454 | -75 | N/A | 4949128 | 1.7057 | 0.39 |

| Method 2 | | | | | | | |
|---|---|---|---|---|---|---|---|
| -284.4 | 8252630 | N/A | -285 | 6548311 | N/A | 1.7043 | 0.31 |
| -289.4 | 8524744 | N/A | -290 | 6820436 | N/A | 1.7043 | 0.31 |
| -294.4 | 8796857 | N/A | -295 | 7092562 | N/A | 1.7043 | 0.31 |
| -299.4 | 9068971 | N/A | -300 | 7364687 | N/A | 1.7043 | 0.31 |
| -304.4 | 9341084 | N/A | -305 | 7636813 | N/A | 1.7043 | 0.31 |

The analogous computations for the ten subsets of the full scan yield similar results as shown in Table 5.8a and 5.8b with and without RMS adjustments, respectively. Here, 3 000 points were adaptively selected as vertices for the meshing. The same offset of 0.6 cm is used to match floor levels. The error trends for the five reference levels are again almost exactly linear, but with different slopes and signs, which was unexpected. Another counterintuitive result is that for data set #3, Method 2 performs considerably better than Method 1, whereas the opposite is true in all other cases. The results presented in Tables 5.7 and 5.8 are plotted in Fig. 5.6 and Fig. 5.7.

Table 5.8a. Processing samples with RMS adjustments for 10 subsets of data.

| Floor Level (cm) | Box 01 3000 points meshed | | Floor Level (cm) | No Box – 01 3000 points meshed | | Box Vol. ($m^3$) | Error (%) |
|---|---|---|---|---|---|---|---|
| | Cut Volume ($cm^3$) | Fill Volume ($cm^3$) | | Cut Volume ($cm^3$) | Fill Volume ($cm^3$) | | |
| **Method 1** | | | | | | | |
| -54.4 | N/A | 4261532 | -55 | N/A | 5962846 | 1.7013 | 0.14 |
| -59.4 | N/A | 3999156 | -60 | N/A | 5701305 | 1.7021 | 0.19 |
| -64.4 | N/A | 3740032 | -65 | N/A | 5442911 | 1.7029 | 0.23 |
| -69.4 | N/A | 3484269 | -70 | N/A | 5187829 | 1.7036 | 0.27 |
| -74.4 | N/A | 3231784 | -75 | N/A | 4935985 | 1.7042 | 0.31 |
| **Method 2** | | | | | | | |
| -284.4 | 8220953 | N/A | -285 | 6497933 | N/A | 1.7230 | 1.41 |
| -289.4 | 8492063 | N/A | -290 | 6768563 | N/A | 1.7235 | 1.44 |
| -294.4 | 8763173 | N/A | -295 | 7039194 | N/A | 1.7240 | 1.47 |
| -299.4 | 9034283 | N/A | -300 | 7309825 | N/A | 1.7245 | 1.50 |
| -304.4 | 9305393 | N/A | -305 | 7580455 | N/A | 1.7249 | 1.53 |
| **Floor Level (cm)** | **Box 02 3000 points meshed** | | **Floor Level (cm)** | **No Box – 02 3000 points meshed** | | **Box Vol. ($m^3$)** | **Error (%)** |
| | **Cut Volume ($cm^3$)** | **Fill Volume ($cm^3$)** | | **Cut Volume ($cm^3$)** | **Fill Volume ($cm^3$)** | | |
| **Method 1** | | | | | | | |
| -54.4 | N/A | 4273449 | -55 | N/A | 5968685 | 1.6952 | -0.22 |
| -59.4 | N/A | 4010479 | -60 | N/A | 5706515 | 1.6960 | -0.17 |
| -64.4 | N/A | 3750721 | -65 | N/A | 5447601 | 1.6969 | -0.12 |
| -69.4 | N/A | 3494477 | -70 | N/A | 5191963 | 1.6975 | -0.09 |
| -74.4 | N/A | 3241553 | -75 | N/A | 4939610 | 1.6981 | -0.06 |
| **Method 2** | | | | | | | |
| -284.4 | 8240311 | N/A | -285 | 6521041 | N/A | 1.7193 | 1.19 |
| -289.4 | 8512090 | N/A | -290 | 6792302 | N/A | 1.7198 | 1.22 |
| -294.4 | 8783870 | N/A | -295 | 7063564 | N/A | 1.7203 | 1.25 |
| -299.4 | 9055649 | N/A | -300 | 7334825 | N/A | 1.7208 | 1.28 |
| -304.4 | 9327429 | N/A | -305 | 7606086 | N/A | 1.7213 | 1.32 |
| **Floor Level (cm)** | **Box 03 3000 points meshed** | | **Floor Level (cm)** | **No Box – 03 3000 points meshed** | | **Box Vol. ($m^3$)** | **Error (%)** |
| | **Cut Volume ($cm^3$)** | **Fill Volume ($cm^3$)** | | **Cut Volume ($cm^3$)** | **Fill Volume\ ($cm^3$)** | | |
| **Method 1** | | | | | | | |
| -54.4 | N/A | 4262099 | -55 | N/A | 5971634 | 1.7095 | 0.62 |

| | | | | | | | |
|---|---|---|---|---|---|---|---|
| -59.4 | N/A | 3999745 | -60 | N/A | 5709339 | 1.7096 | 0.62 |
| -64.4 | N/A | 3740679 | -65 | N/A | 5450296 | 1.7096 | 0.62 |
| -69.4 | N/A | 3484990 | -70 | N/A | 5194479 | 1.7095 | 0.62 |
| -74.4 | N/A | 3232722 | -75 | N/A | 4941982 | 1.7093 | 0.60 |
| **Method 2** | | | | | | | |
| -284.4 | 8221805 | N/A | -285 | 6525009 | N/A | 1.6968 | -0.13 |
| -289.4 | 8492938 | N/A | -290 | 6796411 | N/A | 1.6965 | -0.15 |
| -294.4 | 8764071 | N/A | -295 | 7067813 | N/A | 1.6963 | -0.16 |
| -299.4 | 9035204 | N/A | -300 | 7339216 | N/A | 1.6960 | -0.18 |
| -304.4 | 9306337 | N/A | -305 | 7610618 | N/A | 1.6957 | -0.19 |

| Floor Level (cm) | Box 04 3000 points meshed | | Floor Level (cm) | No Box – 04 3000 points meshed | | Box Vol. ($m^3$) | Error (%) |
|---|---|---|---|---|---|---|---|
| | Cut Volume ($cm^3$) | Fill Volume ($cm^3$) | | Cut Volume ($cm^3$) | Fill Volume ($cm^3$) | | |
| **Method 1** | | | | | | | |
| -54.4 | N/A | 4271003 | -55 | N/A | 5962810 | 1.6918 | -0.42 |
| -59.4 | N/A | 4008232 | -60 | N/A | 5701292 | 1.6931 | -0.35 |
| -64.4 | N/A | 3748770 | -65 | N/A | 5442930 | 1.6942 | -0.28 |
| -69.4 | N/A | 3492708 | -70 | N/A | 5187886 | 1.6952 | -0.22 |
| -74.4 | N/A | 3239950 | -75 | N/A | 4936043 | 1.6961 | -0.17 |
| **Method 2** | | | | | | | |
| -284.4 | 8231735 | N/A | -285 | 6499401 | N/A | 1.7323 | 1.96 |
| -289.4 | 8503279 | N/A | -290 | 6770059 | N/A | 1.7332 | 2.01 |
| -294.4 | 8774822 | N/A | -295 | 7040717 | N/A | 1.7341 | 2.07 |
| -299.4 | 9046365 | N/A | -300 | 7311375 | N/A | 1.7350 | 2.12 |
| -304.4 | 9317908 | N/A | -305 | 7582033 | N/A | 1.7359 | 2.17 |

| Floor Level (cm) | Box 05 3000 points meshed | | Floor Level (cm) | No Box – 05 3000 points meshed | | Box Vol. ($m^3$) | Error (%) |
|---|---|---|---|---|---|---|---|
| | Cut Volume ($cm^3$) | Fill Volume ($cm^3$) | | Cut Volume ($cm^3$) | Fill Volume ($cm^3$) | | |
| **Method 1** | | | | | | | |
| -54.4 | N/A | 4262402 | -55 | N/A | 5964827 | 1.7024 | 0.20 |
| -59.4 | N/A | 3999957 | -60 | N/A | 5702856 | 1.7029 | 0.23 |
| -64.4 | N/A | 3740782 | -65 | N/A | 5444052 | 1.7033 | 0.25 |
| -69.4 | N/A | 3484965 | -70 | N/A | 5188648 | 1.7037 | 0.28 |
| -74.4 | N/A | 3232431 | -75 | N/A | 4936540 | 1.7041 | 0.30 |
| **Method 2** | | | | | | | |
| -284.4 | 8226717 | N/A | -285 | 6513255 | N/A | 1.7135 | 0.85 |
| -289.4 | 8497966 | N/A | -290 | 6784261 | N/A | 1.7137 | 0.87 |
| -294.4 | 8769215 | N/A | -295 | 7055268 | N/A | 1.7139 | 0.88 |
| -299.4 | 9040464 | N/A | -300 | 7326275 | N/A | 1.7142 | 0.89 |
| -304.4 | 9311713 | N/A | -305 | 7597281 | N/A | 1.7144 | 0.91 |

| Floor Level (cm) | Box 06 3000 points meshed | | Floor Level (cm) | No Box – 06 3000 points meshed | | Box Vol. ($m^3$) | Error (%) |
|---|---|---|---|---|---|---|---|
| | Cut Volume ($cm^3$) | Fill Volume ($cm^3$) | | Cut Volume ($cm^3$) | Fill Volume ($cm^3$) | | |
| **Method 1** | | | | | | | |
| -54.4 | N/A | 4260361 | -55 | N/A | 5961267 | 1.7009 | 0.11 |
| -59.4 | N/A | 3998168 | -60 | N/A | 5699518 | 1.7013 | 0.14 |
| -64.4 | N/A | 3739259 | -65 | N/A | 5441135 | 1.7019 | 0.17 |
| -69.4 | N/A | 3483790 | -70 | N/A | 5186043 | 1.7023 | 0.19 |
| -74.4 | N/A | 3231740 | -75 | N/A | 4934184 | 1.7024 | 0.20 |
| **Method 2** | | | | | | | |
| -284.4 | 8215414 | N/A | -285 | 6505609 | N/A | 1.7098 | 0.64 |
| -289.4 | 8486372 | N/A | -290 | 6776368 | N/A | 1.7100 | 0.65 |
| -294.4 | 8757330 | N/A | -295 | 7047127 | N/A | 1.7102 | 0.66 |
| -299.4 | 9028289 | N/A | -300 | 7317886 | N/A | 1.7104 | 0.67 |
| -304.4 | 9299247 | N/A | -305 | 7588644 | N/A | 1.7106 | 0.68 |

| Floor Level (cm) | Box 07 3000 points meshed | | Floor Level (cm) | No Box – 07 3000 points meshed | | Box Vol. ($m^3$) | Error (%) |
|---|---|---|---|---|---|---|---|
| | Cut Volume ($cm^3$) | Fill Volume ($cm^3$) | | Cut Volume ($cm^3$) | Fill Volume ($cm^3$) | | |
| **Method 1** | | | | | | | |
| -54.4 | N/A | 4271016 | -55 | N/A | 5965571 | 1.6946 | -0.26 |
| -59.4 | N/A | 4008232 | -60 | N/A | 5703799 | 1.6956 | -0.20 |
| -64.4 | N/A | 3748786 | -65 | N/A | 5445413 | 1.6966 | -0.14 |
| -69.4 | N/A | 3492744 | -70 | N/A | 5190335 | 1.6976 | -0.08 |
| -74.4 | N/A | 3239954 | -75 | N/A | 4938413 | 1.6985 | -0.03 |
| **Method 2** | | | | | | | |
| -284.4 | 8227652 | N/A | -285 | 6500777 | N/A | 1.7269 | 1.64 |
| -289.4 | 8499110 | N/A | -290 | 6771523 | N/A | 1.7276 | 1.68 |
| -294.4 | 8770568 | N/A | -295 | 7042268 | N/A | 1.7283 | 1.72 |
| -299.4 | 9042025 | N/A | -300 | 7313014 | N/A | 1.7290 | 1.77 |
| -304.4 | 9313483 | N/A | -305 | 7583759 | N/A | 1.7297 | 1.81 |

| Floor Level (cm) | Box 08 3000 points meshed | | Floor Level (cm) | No Box – 08 3000 points meshed | | Box Vol. ($m^3$) | Error (%) |
|---|---|---|---|---|---|---|---|
| | Cut Volume ($cm^3$) | Fill Volume ($cm^3$) | | Cut Volume ($cm^3$) | Fill Volume ($cm^3$) | | |
| **Method 1** | | | | | | | |
| -54.4 | N/A | 4267298 | -55 | N/A | 5960378 | 1.6931 | -0.35 |
| -59.4 | N/A | 4004670 | -60 | N/A | 5698832 | 1.6942 | -0.28 |
| -64.4 | N/A | 3745263 | -65 | N/A | 5440587 | 1.6953 | -0.22 |
| -69.4 | N/A | 3489318 | -70 | N/A | 5185529 | 1.6962 | -0.16 |
| -74.4 | N/A | 3236614 | -75 | N/A | 4933681 | 1.6971 | -0.11 |
| **Method 2** | | | | | | | |
| -284.4 | 8228771 | N/A | -285 | 6501552 | N/A | 1.7272 | 1.66 |
| -289.4 | 8500168 | N/A | -290 | 6772204 | N/A | 1.7280 | 1.70 |
| -294.4 | 8771564 | N/A | -295 | 7042855 | N/A | 1.7287 | 1.75 |
| -299.4 | 9042961 | N/A | -300 | 7313506 | N/A | 1.7295 | 1.79 |
| -304.4 | 9314357 | N/A | -305 | 7584157 | N/A | 1.7302 | 1.84 |

| Floor Level (cm) | Box 09 3000 points meshed | | Floor Level (cm) | No Box – 09 3000 points meshed | | Box Vol. ($m^3$) | Error (%) |
|---|---|---|---|---|---|---|---|
| | Cut Volume ($cm^3$) | Fill Volume ($cm^3$) | | Cut Volume ($cm^3$) | Fill Volume ($cm^3$) | | |
| **Method 1** | | | | | | | |
| -54.4 | N/A | 4267094 | -55 | N/A | 5960493 | 1.6934 | -0.33 |
| -59.4 | N/A | 4004413 | -60 | N/A | 5699025 | 1.6946 | -0.26 |
| -64.4 | N/A | 3745021 | -65 | N/A | 5440726 | 1.6957 | -0.19 |
| -69.4 | N/A | 3489039 | -70 | N/A | 5185678 | 1.6966 | -0.14 |
| -74.4 | N/A | 3236376 | -75 | N/A | 4933842 | 1.6975 | -0.09 |
| **Method 2** | | | | | | | |
| -284.4 | 8230516 | N/A | -285 | 6498934 | N/A | 1.7316 | 1.92 |
| -289.4 | 8501946 | N/A | -290 | 6769537 | N/A | 1.7324 | 1.97 |
| -294.4 | 8773375 | N/A | -295 | 7040141 | N/A | 1.7332 | 2.01 |
| -299.4 | 9044805 | N/A | -300 | 7310745 | N/A | 1.7341 | 2.06 |
| -304.4 | 9316235 | N/A | -305 | 7581348 | N/A | 1.7349 | 2.11 |

| Floor Level (cm) | Box 10 3000 points meshed | | Floor Level (cm) | No Box – 10 3000 points meshed | | Box Vol. ($m^3$) | Error (%) |
|---|---|---|---|---|---|---|---|
| | Cut Volume ($cm^3$) | Fill Volume ($cm^3$) | | Cut Volume ($cm^3$) | Fill Volume ($cm^3$) | | |
| **Method 1** | | | | | | | |
| -54.4 | N/A | 4262054 | -55 | N/A | 5966361 | 1.7043 | 0.31 |
| -59.4 | N/A | 3999659 | -60 | N/A | 5704390 | 1.7047 | 0.34 |
| -64.4 | N/A | 3740525 | -65 | N/A | 5445632 | 1.7051 | 0.36 |
| -69.4 | N/A | 3484706 | -70 | N/A | 5190226 | 1.7055 | 0.38 |
| -74.4 | N/A | 3232200 | -75 | N/A | 4938112 | 1.7059 | 0.41 |
| **Method 2** | | | | | | | |
| -284.4 | 8227650 | N/A | -285 | 6513124 | N/A | 1.7145 | 0.91 |

| | | | | | | | |
|---|---|---|---|---|---|---|---|
| -289.4 | 8498909 | N/A | -290 | 6784156 | N/A | 1.7148 | 0.93 |
| -294.4 | 8770168 | N/A | -295 | 7055189 | N/A | 1.7150 | 0.94 |
| -299.4 | 9041427 | N/A | -300 | 7326221 | N/A | 1.7152 | 0.95 |
| -304.4 | 9312687 | N/A | -305 | 7597253 | N/A | 1.7154 | 0.97 |

Table 5.8b. Processing samples without RMS adjustments for 10 subsets of data.

| Floor Level (cm) | Box – 01 3000 points meshed | | Floor Level (cm) | No Box – 01 3000 points meshed | | Box Vol. ($m^3$) | Error (%) |
|---|---|---|---|---|---|---|---|
| | Cut Volume ($cm^3$) | Fill Volume ($cm^3$) | | Cut Volume ($cm^3$) | Fill Volume ($cm^3$) | | |
| **Method 1** | | | | | | | |
| -54.4 | N/A | 4261449 | -55 | N/A | 5962442 | 1.7010 | 0.12 |
| -59.4 | N/A | 3999093 | -60 | N/A | 5701024 | 1.7019 | 0.17 |
| -64.4 | N/A | 3739939 | -65 | N/A | 5442765 | 1.7028 | 0.23 |
| -69.4 | N/A | 3484207 | -70 | N/A | 5187792 | 1.7036 | 0.27 |
| -74.4 | N/A | 3231730 | -75 | N/A | 4936000 | 1.7043 | 0.31 |
| **Method 2** | | | | | | | |
| -284.4 | 8221086 | N/A | -285 | 6498465 | N/A | 1.7226 | 1.39 |
| -289.4 | 8492196 | N/A | -290 | 6769096 | N/A | 1.7231 | 1.42 |
| -294.4 | 8763306 | N/A | -295 | 7039727 | N/A | 1.7236 | 1.45 |
| -299.4 | 9034416 | N/A | -300 | 7310357 | N/A | 1.7241 | 1.47 |
| -304.4 | 9305526 | N/A | -305 | 7580988 | N/A | 1.7245 | 1.50 |
| **Floor Level (cm)** | **Box – 02 3000 points meshed** | | **Floor Level (cm)** | **No Box – 02 3000 points meshed** | | **Box Vol. ($m^3$)** | **Error (%)** |
| | **Cut Volume ($cm^3$)** | **Fill Volume ($cm^3$)** | | **Cut Volume ($cm^3$)** | **Fill Volume ($cm^3$)** | | |
| **Method 1** | | | | | | | |
| -54.4 | N/A | 4272766 | -55 | N/A | 5968602 | 1.6958 | -0.19 |
| -59.4 | N/A | 4009853 | -60 | N/A | 5706461 | 1.6966 | -0.14 |
| -64.4 | N/A | 3750145 | -65 | N/A | 5447641 | 1.6975 | -0.09 |
| -69.4 | N/A | 3493943 | -70 | N/A | 5192063 | 1.6981 | -0.05 |
| -74.4 | N/A | 3241044 | -75 | N/A | 4939805 | 1.6988 | -0.01 |
| **Method 2** | | | | | | | |
| -284.4 | 8241248 | N/A | -285 | 6521232 | N/A | 1.7200 | 1.24 |
| -289.4 | 8513028 | N/A | -290 | 6792494 | N/A | 1.7205 | 1.27 |
| -294.4 | 8784807 | N/A | -295 | 7063755 | N/A | 1.7211 | 1.30 |
| -299.4 | 9056587 | N/A | -300 | 7335016 | N/A | 1.7216 | 1.33 |
| -304.4 | 9328366 | N/A | -305 | 7606277 | N/A | 1.7221 | 1.36 |
| **Floor Level (cm)** | **Box – 03 3000 points meshed** | | **Floor Level (cm)** | **No Box – 03 3000 points meshed** | | **Box Vol. ($m^3$)** | **Error (%)** |
| | **Cut Volume ($cm^3$)** | **Fill Volume ($cm^3$)** | | **Cut Volume ($cm^3$)** | **Fill Volume ($cm^3$)** | | |
| **Method 1** | | | | | | | |
| -54.4 | N/A | 4260361 | -55 | N/A | 5970773 | 1.7104 | 0.67 |
| -59.4 | N/A | 3997963 | -60 | N/A | 5708439 | 1.7105 | 0.68 |
| -64.4 | N/A | 3738837 | -65 | N/A | 5449374 | 1.7105 | 0.68 |
| -69.4 | N/A | 3483089 | -70 | N/A | 5193539 | 1.7105 | 0.67 |
| -74.4 | N/A | 3230873 | -75 | N/A | 4941089 | 1.7102 | 0.66 |
| **Method 2** | | | | | | | |
| -284.4 | 8223780 | N/A | -285 | 6526010 | N/A | 1.6978 | -0.07 |
| -289.4 | 8494913 | N/A | -290 | 6797412 | N/A | 1.6975 | -0.09 |

| | | | | | | | |
|---|---|---|---|---|---|---|---|
| -294.4 | 8766045 | N/A | -295 | 7068814 | N/A | 1.6972 | -0.10 |
| -299.4 | 9037178 | N/A | -300 | 7340217 | N/A | 1.6970 | -0.12 |
| -304.4 | 9308311 | N/A | -305 | 7611619 | N/A | 1.6967 | -0.14 |

| Floor Level (cm) | Box – 04 3000 points meshed | | Floor Level (cm) | No Box – 04 3000 points meshed | | Box Vol. ($m^3$) | Error (%) |
|---|---|---|---|---|---|---|---|
| | Cut Volume ($cm^3$) | Fill Volume ($cm^3$) | | Cut Volume ($cm^3$) | Fill Volume ($cm^3$) | | |
| **Method 1** | | | | | | | |
| -54.4 | N/A | 4269038 | -55 | N/A | 5961613 | 1.6926 | -0.38 |
| -59.4 | N/A | 4006325 | -60 | N/A | 5700140 | 1.6938 | -0.31 |
| -64.4 | N/A | 3746882 | -65 | N/A | 5441815 | 1.6949 | -0.24 |
| -69.4 | N/A | 3490847 | -70 | N/A | 5186813 | 1.6960 | -0.18 |
| -74.4 | N/A | 3238087 | -75 | N/A | 4934977 | 1.6970 | -0.12 |
| **Method 2** | | | | | | | |
| -284.4 | 8233785 | N/A | -285 | 6500719 | N/A | 1.7331 | 2.01 |
| -289.4 | 8505328 | N/A | -290 | 6771377 | N/A | 1.7340 | 2.06 |
| -294.4 | 8776871 | N/A | -295 | 7042035 | N/A | 1.7348 | 2.11 |
| -299.4 | 9048414 | N/A | -300 | 7312693 | N/A | 1.7357 | 2.16 |
| -304.4 | 9319957 | N/A | -305 | 7583351 | N/A | 1.7366 | 2.21 |

| Floor Level (cm) | Box – 05 3000 points meshed | | Floor Level (cm) | No Box – 05 3000 points meshed | | Box Vol. ($m^3$) | Error (%) |
|---|---|---|---|---|---|---|---|
| | Cut Volume ($cm^3$) | Fill Volume ($cm^3$) | | Cut Volume ($cm^3$) | Fill Volume ($cm^3$) | | |
| **Method 1** | | | | | | | |
| -54.4 | N/A | 4260880 | -55 | N/A | 5965368 | 1.7045 | 0.32 |
| -59.4 | N/A | 3998463 | -60 | N/A | 5703432 | 1.7050 | 0.35 |
| -64.4 | N/A | 3739316 | -65 | N/A | 5444635 | 1.7053 | 0.37 |
| -69.4 | N/A | 3483545 | -70 | N/A | 5189291 | 1.7057 | 0.40 |
| -74.4 | N/A | 3231086 | -75 | N/A | 4937214 | 1.7061 | 0.42 |
| **Method 2** | | | | | | | |
| -284.4 | 8228148 | N/A | -285 | 6512812 | N/A | 1.7153 | 0.96 |
| -289.4 | 8499397 | N/A | -290 | 6783818 | N/A | 1.7156 | 0.98 |
| -294.4 | 8770646 | N/A | -295 | 7054825 | N/A | 1.7158 | 0.99 |
| -299.4 | 9041894 | N/A | -300 | 7325832 | N/A | 1.7161 | 1.00 |
| -304.4 | 9313143 | N/A | -305 | 7596838 | N/A | 1.7163 | 1.02 |

| Floor Level (cm) | Box – 06 3000 points meshed | | Floor Level (cm) | No Box – 06 3000 points meshed | | Box Vol. ($m^3$) | Error (%) |
|---|---|---|---|---|---|---|---|
| | Cut Volume ($cm^3$) | Fill Volume ($cm^3$) | | Cut Volume ($cm^3$) | Fill Volume ($cm^3$) | | |
| **Method 1** | | | | | | | |
| -54.4 | N/A | 4259753 | -55 | N/A | 5960251 | 1.7005 | 0.09 |
| -59.4 | N/A | 3997557 | -60 | N/A | 5698502 | 1.7009 | 0.11 |
| -64.4 | N/A | 3738646 | -65 | N/A | 5440078 | 1.7014 | 0.14 |
| -69.4 | N/A | 3483114 | -70 | N/A | 5184958 | 1.7018 | 0.17 |
| -74.4 | N/A | 3231027 | -75 | N/A | 4933064 | 1.7020 | 0.18 |
| **Method 2** | | | | | | | |
| -284.4 | 8216055 | N/A | -285 | 6506632 | N/A | 1.7094 | 0.61 |
| -289.4 | 8487013 | N/A | -290 | 6777390 | N/A | 1.7096 | 0.63 |
| -294.4 | 8757971 | N/A | -295 | 7048149 | N/A | 1.7098 | 0.64 |
| -299.4 | 9028929 | N/A | -300 | 7318908 | N/A | 1.7100 | 0.65 |
| -304.4 | 9299887 | N/A | -305 | 7589667 | N/A | 1.7102 | 0.66 |

| Floor Level (cm) | Box – 07 3000 points meshed | | Floor Level (cm) | No Box – 07 3000 points meshed | | Box Vol. (m^3) | Error (%) |
|---|---|---|---|---|---|---|---|
| | Cut Volume ($cm^3$) | Fill Volume ($cm^3$) | | Cut Volume ($cm^3$) | Fill Volume ($cm^3$) | | |
| **Method 1** | | | | | | | |
| -54.4 | N/A | 4270027 | -55 | N/A | 5967066 | 1.6970 | -0.12 |
| -59.4 | N/A | 4007149 | -60 | N/A | 5705331 | 1.6982 | -0.05 |
| -64.4 | N/A | 3747619 | -65 | N/A | 5446837 | 1.6992 | 0.01 |
| -69.4 | N/A | 3491559 | -70 | N/A | 5191587 | 1.7000 | 0.06 |
| -74.4 | N/A | 3238763 | -75 | N/A | 4939506 | 1.7007 | 0.10 |
| **Method 2** | | | | | | | |
| -284.4 | 8228700 | N/A | -285 | 6499495 | N/A | 1.7292 | 1.78 |
| -289.4 | 8500158 | N/A | -290 | 6770240 | N/A | 1.7299 | 1.82 |
| -294.4 | 8771616 | N/A | -295 | 7040986 | N/A | 1.7306 | 1.86 |
| -299.4 | 9043074 | N/A | -300 | 7311731 | N/A | 1.7313 | 1.90 |
| -304.4 | 9314531 | N/A | -305 | 7582476 | N/A | 1.7321 | 1.95 |

| Floor Level (cm) | Box – 08 3000 points meshed | | Floor Level (cm) | No Box – 08 3000 points meshed | | Box Vol. ($m^3$) | Error (%) |
|---|---|---|---|---|---|---|---|
| | Cut Volume ($cm^3$) | Fill Volume ($cm^3$) | | Cut Volume ($cm^3$) | Fill Volume ($cm^3$) | | |
| **Method 1** | | | | | | | |
| -54.4 | N/A | 4266799 | -55 | N/A | 5960564 | 1.6938 | -0.31 |
| -59.4 | N/A | 4004200 | -60 | N/A | 5699036 | 1.6948 | -0.25 |
| -64.4 | N/A | 3744766 | -65 | N/A | 5440759 | 1.6960 | -0.18 |
| -69.4 | N/A | 3488822 | -70 | N/A | 5185617 | 1.6968 | -0.13 |
| -74.4 | N/A | 3236154 | -75 | N/A | 4933635 | 1.6975 | -0.09 |
| **Method 2** | | | | | | | |
| -284.4 | 8229390 | N/A | -285 | 6501323 | N/A | 1.7281 | 1.71 |
| -289.4 | 8500787 | N/A | -290 | 6771974 | N/A | 1.7288 | 1.75 |
| -294.4 | 8772183 | N/A | -295 | 7042625 | N/A | 1.7296 | 1.80 |
| -299.4 | 9043580 | N/A | -300 | 7313276 | N/A | 1.7303 | 1.84 |
| -304.4 | 9314976 | N/A | -305 | 7583927 | N/A | 1.7310 | 1.89 |

| Floor Level (cm) | Box – 09 3000 points meshed | | Floor Level (cm) | No Box – 09 3000 points meshed | | Box Vol. ($m^3$) | Error (%) |
|---|---|---|---|---|---|---|---|
| | Cut Volume ($cm^3$) | Fill Volume ($cm^3$) | | Cut Volume ($cm^3$) | Fill Volume ($cm^3$) | | |
| **Method 1** | | | | | | | |
| -54.4 | N/A | 4266962 | -55 | N/A | 5960031 | 1.6931 | -0.35 |
| -59.4 | N/A | 4004213 | -60 | N/A | 5698588 | 1.6944 | -0.27 |
| -64.4 | N/A | 3744720 | -65 | N/A | 5440279 | 1.6956 | -0.20 |
| -69.4 | N/A | 3488715 | -70 | N/A | 5185259 | 1.6965 | -0.14 |
| -74.4 | N/A | 3236064 | -75 | N/A | 4933476 | 1.6974 | -0.09 |
| **Method 2** | | | | | | | |
| -284.4 | 8230733 | N/A | -285 | 6499629 | N/A | 1.7311 | 1.89 |
| -289.4 | 8502163 | N/A | -290 | 6770233 | N/A | 1.7319 | 1.94 |
| -294.4 | 8773593 | N/A | -295 | 7040837 | N/A | 1.7328 | 1.99 |
| -299.4 | 9045023 | N/A | -300 | 7311440 | N/A | 1.7336 | 2.04 |
| -304.4 | 9316452 | N/A | -305 | 7582044 | N/A | 1.7344 | 2.08 |

| Floor Level (cm) | Box – 10 3000 points meshed | | Floor Level (cm) | No Box – 10 3000 points meshed | | Box Vol. ($m^3$) | Error (%) |
|---|---|---|---|---|---|---|---|
| | Cut Volume ($cm^3$) | Fill Volume ($cm^3$) | | Cut Volume ($cm^3$) | Fill Volume ($cm^3$) | | |
| **Method 1** | | | | | | | |
| -54.4 | N/A | 4261363 | -55 | N/A | 5965047 | 1.7037 | 0.28 |
| -59.4 | N/A | 3999034 | -60 | N/A | 5703179 | 1.7041 | 0.30 |
| -64.4 | N/A | 3739911 | -65 | N/A | 5444506 | 1.7046 | 0.33 |
| -69.4 | N/A | 3484071 | -70 | N/A | 5189127 | 1.7051 | 0.36 |
| -74.4 | N/A | 3231613 | -75 | N/A | 4936995 | 1.7054 | 0.38 |
| **Method 2** | | | | | | | |
| -284.4 | 8228488 | N/A | -285 | 6514594 | N/A | 1.7139 | 0.88 |
| -289.4 | 8499748 | N/A | -290 | 6785626 | N/A | 1.7141 | 0.89 |
| -294.4 | 8771007 | N/A | -295 | 7056658 | N/A | 1.7143 | 0.90 |
| -299.4 | 9042266 | N/A | -300 | 7327690 | N/A | 1.7146 | 0.92 |
| -304.4 | 9313525 | N/A | -305 | 7598723 | N/A | 1.7148 | 0.93 |

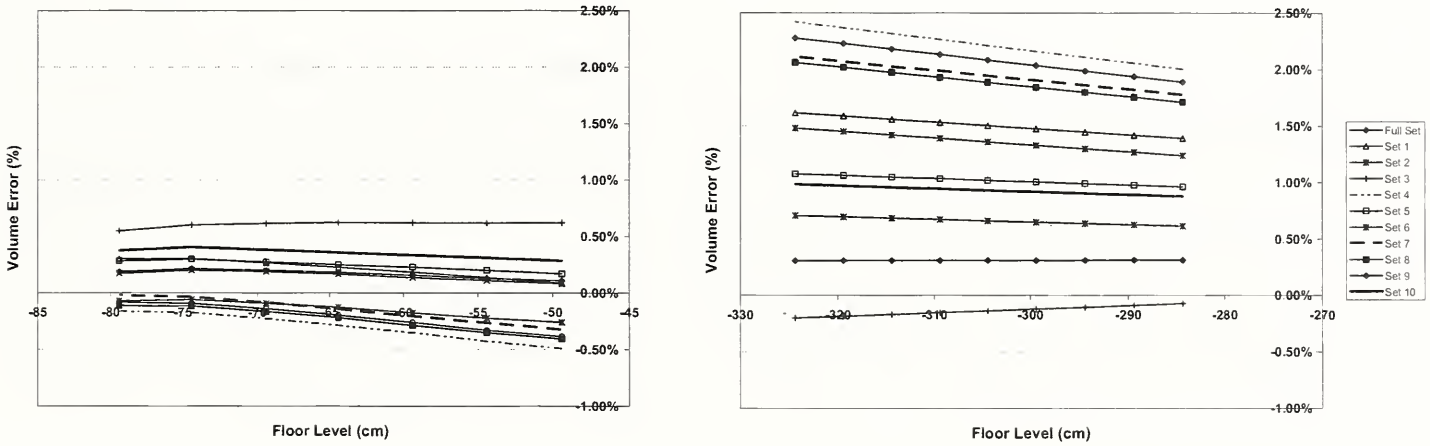


a. Method 1

b. Method 2

Figure 5.6: Experiment 4 without RMS adjustments: Volume error for full data set and 10 subsets.

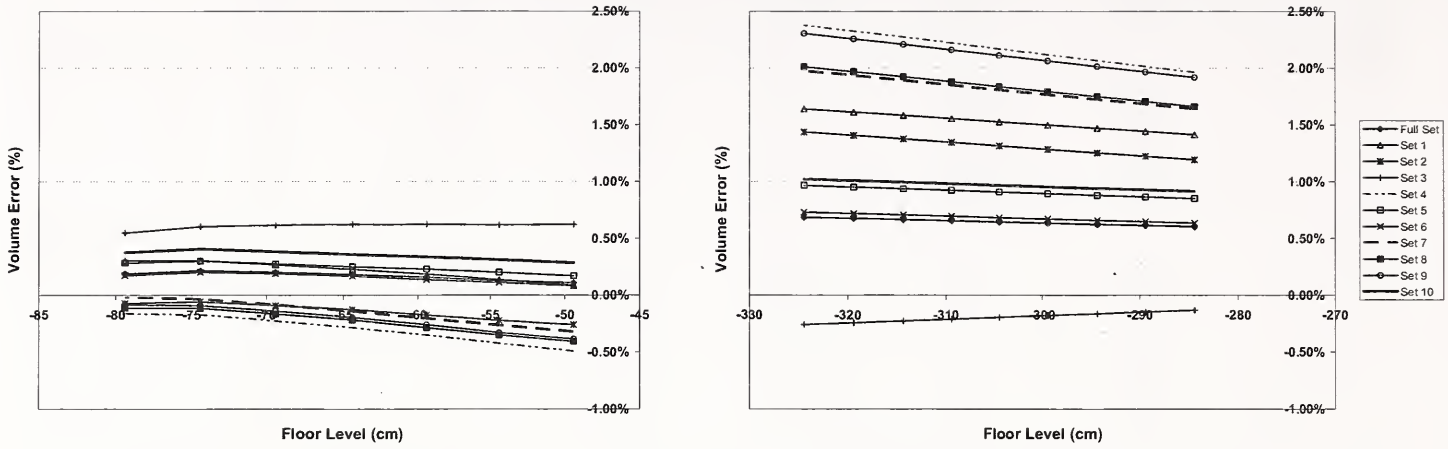


a. Method 1

b. Method 2

Figure 5.7. Experiment 4 with RMS adjustments: Volume error for full data set and 10 subsets.

A summary of the results for Experiment 4 is given in Table 5.9. In this table, the mean and the standard deviation for volume computations were associated with reference level pair -74.4 cm, 75.0 cm is selected as the result of Method 1, and the volume associated with the floor pair -284.4 cm, 285.0 cm as the result of Method 2. In conjunction with either method, the RMS adjustment did not result in a significant improvement. In fact, for the full data set, the RMS adjustment increased the volume error for all floor levels chosen for Method 1, while yielding improvements for all levels for Method 2. With and without RMS adjustments, the volume error using Method 1 remained below the standard deviation. For Method 2, the volume error is about double the standard deviation. In nine out of ten instances, the values provided by Method 2 overestimate the "true" volume of 1.6990 $m^3$, indicating an unresolved bias error.

Table 5.9. Summary of Experiment 4 results.

| Data Sub-Set | Volume ($m^3$) | | | |
|---|---|---|---|---|
| | No RMS | | RMS | |
| | Method 1 | Method 2 | Method 1 | Method 2 |
| 1 | 1.704 | 1.723 | 1.704 | 1.723 |
| 2 | 1.699 | 1.720 | 1.698 | 1.719 |
| 3 | 1.710 | 1.698 | 1.709 | 1.697 |
| 4 | 1.697 | 1.733 | 1.696 | 1.732 |
| 5 | 1.706 | 1.715 | 1.704 | 1.713 |
| 6 | 1.702 | 1.709 | 1.702 | 1.710 |
| 7 | 1.701 | 1.729 | 1.698 | 1.727 |
| 8 | 1.697 | 1.728 | 1.697 | 1.727 |
| 9 | 1.697 | 1.731 | 1.697 | 1.732 |
| 10 | 1.705 | 1.714 | 1.706 | 1.715 |
| **Average ($m^3$)** | 1.702 | 1.720 | 1.701 | 1.719 |
| **Std. Dev. ($m^3$)** | 0.0045 | 0.011 | 0.0045 | 0.011 |
| **Volume Error ($m^3$)** | 0.003 | 0.021 | 0.002 | 0.020 |
| **Vol. Error (%)** | 0.17 | 1.24 | 0.14 | 1.21 |

# 6. SUMMARY AND CONCLUSIONS

This report describes experiments conducted to examine the performance and accuracy of TIN techniques for volume determination. The TIN technique is a technique for meshing 3D point clouds in order to represent them by surfaces.

Five pairs of LADAR scans were taken at five specified data densities. For each such density setting, a plywood screen (Fig. 1.1) was scanned with and without a plywood box of known dimensions. The volume of the box was then derived by several alternate procedures as the difference of volumes associated with each pair of scans, respectively. Four experimental procedures for volume determination were examined. Within each such experiment, alternate options and parameter settings were explored.

Experiment 1 was based on the two scans of highest density only. The key parameter to be varied was the number of data points specified to be automatically selected as vertices of the TIN surfaces representing the two point clouds, respectively. This parameter determines the coarseness or resolution of the resulting TIN surface. Varying the number of bins used for constructing an initial triangulation provided a means for examining alternate TIN surfaces. Experiment 1 produced an unexpected result in the volume calculations: for small numbers of vertices and, therefore, coarser TIN surfaces, volumes tend to be overestimated. As the number of vertices increases, the volumes decrease in a regular fashion. The most accurate volumes were thus found when only about 1/3 of the data points were incorporated as vertices. There is yet no evidence whether this observation holds true in general. Nevertheless, for the subsequent experiments, the vertex ratio has been fixed at 1/3.

In Experiment 2, volume calculations for different densities were compared. As expected, the volumes calculated for the highest density setting were the most accurate, and the ones based on the lowest density setting the least accurate. Inexplicably, however, the third highest density setting performed better than the second highest density setting. This phenomenon persisted after triangulation adjustments were used to improve the RMS and ASD measures-of-fit of the point clouds by the respective surfaces.

Experiment 3 was designed to estimate standard errors. The "true" box volume of 1.6990 $m^3$ was reproduced roughly within three standard deviations with volume errors less than 2 %. In all cases, the true volume was underestimated, suggesting bias inherent in the experimental set-up. The underestimation was increased rather than mitigated by the application of a median filter.

Experiment 4 was also designed to estimate standard errors. The objective of Experiment 4 was to examine the effect of defining TIN surfaces in the direction of the scan rather than with reference to a horizontal footprint plane – the procedure used in the previous experiments. In addition, a difference scheme was employed to determine reference elevation levels. Two methods, Method 1 and Method 2, were implemented; the first based on determining fill volumes, the second on cut volumes. Method 1 provided the most exact volume measurements, with errors below 0.2 % and within the standard deviation of 0.004 $m^3$. Method 2 overestimated the "true" volume for all but one of the ten data subsets. The reason for this apparent bias is not

understood. The most meaningful comparison is with Experiment 3, in which the same procedure for estimating standard errors was followed. For Method 1, a definite improvement of volume accuracy was observed, while the results of Method 2 were comparable.

Several procedures for post-processing the TIN surfaces were explored. Minimizing the RMS error of the surface representations – the "elevation adjustment" – was used as an option in all experiments. The option described as "triangulation adjustment" was examined in Experiment 2. Both of these post-processing adjustments improved the accuracy of representation as gauged by specified measures-of-fit; however, these improvements only sporadically translated into improvements of volume accuracy.

The noise level of the scans is estimated to correspond to a standard deviation of roughly 2 cm. A statistical analysis of what accuracy can be realistically expected given this level of noise is planned.

To provide an idea as to the kind of accuracies and uncertainties to expect for volume determinations from LADAR scans, representative volume figures are shown in Table 6.1. They reflect an arbitrary decision to choose approximately 1/3 of the data points as vertices of TIN surfaces for which cut/fill volumes are determined, from which a box volume is subsequently derived. The values and "uncertainties" listed for Experiments 1 and 2 are simply the values over which the available measurements were ranging, expressed by their respective midpoints and maximum deviations. The latter have no statistical meaning. In Experiments 3 and 4, expected values and standard deviations have been calculated for random subsets of the data.

Table 6.1. Summary of Volumes and Uncertainties.

| Experiment | Description | Volume ($m^3$) | | |
|---|---|---|---|---|
| | | Definition | w/ RMS | w/o RMS |
| 1 | Density 1 (Highest) | Mid. range val. ± range limit | 1.6997 ± 0.0023 | 1.701 ± 0.00215 |
| 2 | Density 1 (Highest) | Mid. range val. ± range limit | 1.69640 ± 0.0070 | NA |
| | Density 2 | Mid. range val. ± range limit | 1.67215 ± 0.00105 | NA |
| | Density 3 | Mid. range val. ± range limit | 1.69595 ± 0.00125 | NA |
| | Density 4 | Mid. range val. ± range limit | 1.67680 ± 0.0010 | NA |
| | Density 5 (Lowest) | Mid. range val. ± range limit | 1.63035 ± 0.00425 | NA |
| 3 | Density 1, no filter | Avg. val. ± std. dev. | 1.678 ± 0.0086 | 1.681 ± 0.0094 |
| 4 | Density 1, Method 1 | Avg. val. ± std. dev. | 1.701 ± 0.0045 | 1.702 ± 0.0045 |
| | | | | |
| | | "True" Volume | 1.6990 | |

## REFERENCES


**Cheok, G. S., Lipman, R. R., Witzgall, C., Bernal, J., and Stone, W. C. [2000]**, "NIST Construction Automation Program Report No. 4: Non-Intrusive Scanning Technology for Construction Status Determination," *NISTIR 6457*, National Institute of Standards and Technology, Gaithersburg, MD, January.

**Delaunay, C. [1934]**, "Sur la sphere vide," *Bull. Acad. Sci. USSR* (VII), Classe Sci. Mat., pp. 793-800.

**Edelsbrunner, H., D. G. Kirkpatrick, and R. Seidel [1983]**, "On the Shape of a Set of Points in the Plane," *IEEE Trans. Inform. Theory,* 29, pp. 551-559.

**Lawson, C.L. [1977]**, "Software for $C^1$ surface interpolation," *Mathematical Software III*, J.R. Rice (Ed.), Academic Press, New York, pp. 161-194.

**Peucker, T. K., R. J. Fowler, J. J. Little, and D. M. Mark [1976]**, "Digital Representation of Three Dimensional Surfaces by Triangulated Irregular Networks (TIN)" *Technical Report* 10, Office of Naval Research, Geography Programs.

**Peucker, T. K., R. J. Fowler, J. J. Little, and D. M. Mark [1978]**, "The Triangulated Irregular Network." *Proceedings of the Digital Terrain Model Symposium*, St. Louis, MO, pp. 516-532.

**Witzgall, C., and Cheok, G. S. [2001]**, "Registering 3D Point Clouds: An Experimental Evaluation", *NISTIR 6743*, National Institute of Standards and Technology, Gaithersburg, MD, May.

**Witzgall, C., Bernal, J., and Cheok, G. S. [2004]**, "TIN Techniques for Data Analysis and Surface Construction", *NISTIR 7078*, National Institute of Standards and Technology, Gaithersburg, MD, January.